T-3934

SOLAR PHOTODECOMPOSITION OF DILUTE ORGANICS IN AQUEOUS STREAMS

BY

SHAHAB ALAM

T-3934

A thesis submitted to the Faculty and the Board of Trustees of the Colorado School of Mines in partial fulfillment of the requirements for the degree of Master of Science (Chemical and Petroleum-Refining Engineering).

Golden, Colorado

Date: August 20, 1990

Signed: S. L. Alam
Shahab Alam

Approved: Victor F. Yesavage
Prof. V.F. Yesavage
Thesis Advisor

Golden, Colorado

Date: 8/20/90

Dr. R.C. Nix
Co-Advisor

Dr. Robert M. Baldwin
Professor and Head,
Chemical Engineering
and Petroleum Refining department.

ABSTRACT

A series of laboratory and pilot plant runs were performed to investigate the techno-economic feasibility of solar photodetoxification of water contaminated with textile dyes. The objective of this research work was the development of a pollution control process, which uses solar energy to enhance industrial waste management and to improve the water quality for the use of mankind.

Kinetic studies were conducted in one sun (the normal solar energy, which we receive at ground level on a clear day at noon), as well as under concentrated (using focusing reflectors) radiation conditions. Two kinetic models, which best fit our experimental data were proposed - one is applicable for high contaminant level, while the other is for low concentration of solute.

The effects of changing process variables such as, catalyst loading and impurities, temperature, addition of oxidant, initial concentration of contaminant and variation in light intensity etc. were also investigated.

On the basis of this study, it is possible for the industrialists, especially the textile industry, to make

plans for improving their water quality either for reuse or for safe disposal into main city streams, provided that abundant sunshine is available in those areas.

TABLE OF CONTENTS

TABLE OF CONTENTS (cont.)

TABLE OF CONTENTS (cont.)

LIST OF FIGURES

LIST OF FIGURES (cont.)

LIST OF FIGURES (cont.)

LIST OF TABLES

ACKNOWLEDGMENTS

First of all I would like to thank my thesis advisor, Prof. V.F. Yesavage and co-advisor, Dr. Gerry Nix for their valuable guidance from time to time during the experimental work, as well as in the preparation of this report. I appreciate the efforts of my thesis committee members Prof. Sami, Selim and Prof. R.M. Baldwin.

My thanks are also due to Solar Energy Research Institute (SERI) and their staff for their cooperation during my experimental work on the pilot plant.

I would also very much appreciate my sponsor, the Ministry of Science and Technology, Government of Pakistan, who granted me the scholarship towards the completion of the Master's degree.

Finally I would appreciate my wife Lubna and kids Saad and Samya for their patience during the preparation of this thesis report.

INTRODUCTION

Due to the ever-increasing contamination of the natural resources of water, the reuse of treated municipal wastewater for crop irrigation, for ground water recharge, or even for potable purposes, has become a real necessity for countries of the arid and semi arid zones. The reuse of effluents for crop irrigation requires that they neither constitute any hazard for people working in the irrigated fields or for those people consuming the agricultural products. Such requirements can be fulfilled by disinfection and detoxification of waste water effluents.

For disinfection of drinking water, chlorination has been widely used in the world. Nowadays, there is increasing pollution of water sources by organic and inorganic compounds. During conventional chlorination of drinking water, dissolved organic molecules can be chlorinated. Many of these chlorinated molecules are toxic or suspected carcinogens, even in trace quantities.

Toxic waste clean-up is a concern to all levels of government and will affect directly or indirectly every citizen and industrial concern. Mostly conventional inciner-

ation, filtration, adsorption and air transfer technologies are used to clean-up the water and make it suitable for the use of mankind. But all these water treatment processes require fuel or electricity, which in turn increases the cost of the overall process.

As indicated earlier, all conventional processes of water purification are energy consuming, even the newly developed reverse osmosis, which is comparatively energy intensive, requires high hydraulic pressures and pumping energy to offset osmotic pressure. Moreover most of the conventional water treatment processes are non-destructive, i.e., they leave a hazardous waste, which can not be directly landfilled.

In the solar detoxification process, U.V. or near U.V. rays (in the region of 200-380 n.m.) are used in the presence of a photo-active catalyst TiO_2 in order to demineralize the toxic waste. Figure 1 presents a block diagram for this newly developed photocatalytic decomposition process. In my present study of solar photodecomposition process, emphasis has been given on the treatment of textile dyes. The problem of textile-waste treatment is one of the most complicated of industrial-waste treatment, mainly

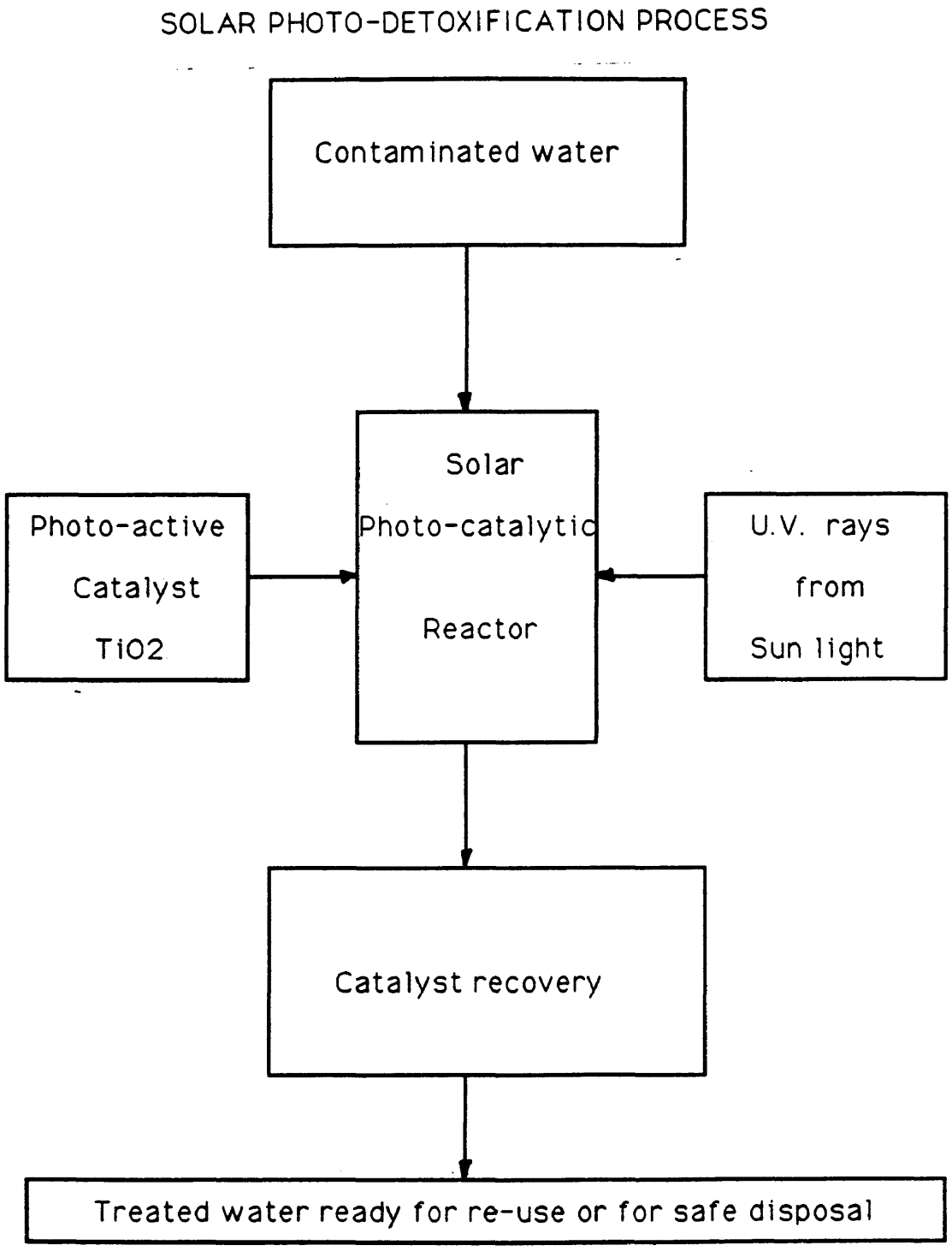

Fig. 1: Block diagram for solar photo-catalytic decomposition process.

because of the extreme variation in textile manufacturing processes. Textile wastes are as varied as the kinds and colors of goods produced by the mill.

Most of my experimental runs were conducted on direct red-79 dye and a few on blue-80 dye that were considered to be model compounds in a typical textile waste. Most of the conventional textile wastewater treatment processes are energy intensive and involve high capital investments. Our proposed process of water purification, which is destructive in nature (it does not leave any residue for further processing), is capable of treating textile dyeing and finishing plant wastes and recovering about 95-99% of the water, which can be reused in the dyeing and finishing plant.

The proposed solar water decontamination process is simple and uses a small amount of conventional fuel derived energy. It offers the following advantages over conventional methods of water purification:

i). Process simplicity.

ii). Shortened treatment time.

iii). Fewer by-products.

iv). Low energy consumption, especially in case of a stand-alone Solar power system.

v). Less maintenance and manpower required.

LITERATURE REVIEW

The phenomenon of heterogeneous solar photocatalysis is often observed in the oxidation of older exterior house paints, a process in which titanium dioxide pigment particles in the paint use part of the sun's energy to oxidize the organic components of the film. This deterioration is now minimized by coating these semiconductor pigment particles with a thin layer of a more photo-inactive oxide such as alumina. Recent literature suggests that certain illuminated semiconductor oxides are "photocatalysts", for more desirable reactions than paint degradation (1).

Photocatalytic effects of semiconductors have been of much interest from the view point of solar energy utilization (2). They have been applied not only to produce useful chemicals, but also to convert pollutants in waste streams to innocuous or less harmful forms. An example is heterogeneous photocatalysis of some n-type semiconductors such as TiO_2 for oxidation of an aqueous solution of phenol. In dilute aqueous solutions, halogenated hydrocarbons such as trichloromethane, trichloroethylene, chlorinated benzenes, PCBs, carbon tetrachloride, perchloroethylene, chloroform

and 1,2-dibromoethane are completely converted to yield less harmful products(4-12). Okamoto et. al. (2) used sunlight to produce the photocatalytic activity of TiO_2 (catalyst) on the reduction of phenol concentration. The experiments were carried out in August in Ube, Japan located in latitude 34^o north. The temperature of the reaction solution was in the range of 30 to 55^oC. The weather was clear to partly cloudy. They observed that the decomposition process obeyed first order reaction kinetics for [phenol].

$$\ln([\text{phenol}]/[\text{phenol}]_o) = -k_{ap}t \qquad (1)$$

Where:

$[\text{phenol}]_o$ is the initial concentration of phenol.

k_{ap} is the apparent first order rate constant.

t is the reaction time.

TiO_2 (anatase) was found photochemically active in aqueous solutions, whereas TiO_2 (rutile) was observed to be inactive. It was interesting from the viewpoint of waste water treatment that phenol was completely mineralized to CO_2 and H_2O in the presence of anatase TiO_2 powder under solar irradiation without either aeration or mixing of the solution. The complete decomposition of phenol seemed to be expressed as follows:

$$C_6H_5OH + 7O_2 \text{ ----> } 6CO_2 + 3H_2O \qquad (2)$$

The same authors further determined that the reaction mechanism was not a simple first order one (3).

Chloroform is a suspected carcinogen and is the major haloform produced from organic matter during the disinfection of municipal waters by chlorination. The degradation of chloroform by photo-assisted heterogeneous catalysis in dilute aqueous suspensions of TiO_2 was studied by Pruden and Ollis (4). They reported the complete mineralization of trichloromethane (chloroform) to hydrogen chloride ion and carbon dioxide by dilute aqueous suspensions (0.1 wt%) of a heterogeneous photoassisted catalyst, titanium dioxide. In the presence of both TiO_2 slurries and near-UV illumination, $CHCl_3$ was rapidly dehalogenated, while in the presence of either illumination or TiO_2 alone, no $CHCl_3$ disappearance or chloride production was observed. The stoichiometry for this heterogeneous photocatalytic conversion is written as:

$$CHCl_3 + H_2O + 1/2\ O_2 \text{ -----> } 3HCl + CO_2 \qquad (3)$$

They observed first order reaction kinetics for both chloroform degradation and chloride production (4). The same researchers also studied the degradation of trichloroethylene (TCE) in water using photoassisted heteroge-

neous catalyst TiO_2. The reaction is written as:

$$CCl_2CClH + 4H_2O \text{ -----> } 2CO_2 + 3HCl + 3H_2 \quad (4)$$

The specific rate for apparent first-order surface decomposition of TCE at constant intensity with chloride competition for the active site was expressed in terms of Langmuir-Hinshelwood kinetics as:

$$-r_{TCE} = k_{TCE}\theta^*_{TCE} \quad (5)$$

where the surface coverage of TCE, θ^*_{TCE}, is

$$\theta^*_{TCE} = \frac{K_{TCE}\theta_{TCE}}{1 + K_{TCE}[TCE] + K_{Cl}[Cl]^-} \quad (6)$$

Where:

k_{TCE} in eq.5 is the surface rate constant.

K_{TCE} is the adsorption co-efficient for TCE.

[TCE] is the concentration of TCE.

K_{Cl} is the adsorption coefficient for chloride.

Equations (5) and (6) were combined, inverted and rearranged to obtain kinetic parameters.

Some recent work done in the field of photocatalytic oxidation of organic is by Mathews, R.W. (13). He investigated the kinetics of photooxidation to CO_2 of 22 organic solutes over a UV illuminated film of Degussa P25 titanium dioxide over a 100-fold concentration range for each solute, generally from about 1 to 100 mg/lit. In the previous stud-

ies by Mathews and other researchers, usually the titanium dioxide has been present as a powder suspension and the destruction of compounds has been studied using a closed system. But in his recent study (13), it was reported that titanium dioxide could be readily attached to glass surfaces allowing the TiO_2 to be illuminated as a stationary phase with water passing over the catalyst. Thus open system continuous operation without discrete catalyst separation steps is possible.

Mathews observed that the adsorption of compounds on TiO_2 follows a Langmuir adsorption isotherm. Thus a strongly adsorbed solute may undergo destruction at a significant rate at parts per million concentrations in the surrounding solution. As the plots for all of the 22 solutes in his experiments were closely approximated by curves having the shape of Langmuir adsorption isotherms, the data set for each solute were treated by the method of least squares assuming that the data were described by the expression:

$$R = \frac{Kk1[s]^{o}}{1 + k1[s]^{o}} \qquad (7)$$

Where:

R is the rate of oxidation of the solute to CO_2.

k_1 is the adsorption co-efficient.

K is the reaction rate constant.

$[S]^o$ is the initial concentration of the solute.

He postulated that both oxygen and the organic solutes are adsorbed at different sites on the surface of the TiO_2. He also assumed that the rate determining step is the reaction between the primary oxidizing species and the organic solute, S. In terms of Langmuir-Hinshelwood kinetics, he expressed the second order decomposition rate at the surface forming CO_2 as:

$$R = k^1\theta_{o2}\theta_s \qquad (8)$$

Where:

k^1 is the reaction rate constant.

θo_2 is the fraction of sites covered by oxygen.

θ_s is the fraction of sites covered by organic solutes.

Because in his experiment, the initial oxygen pressure was the ambient air-equilibrated value, θo_2 may be regarded as constant and expression (8) can be written as:

$$R = k^{11}\theta_s \qquad (9)$$

where the fraction of sites covered by organic solute, θ_s, can be expressed as:

$$\theta_s = \frac{k_1[S]}{1 + k1[S] + \sum_i k_i[I_i]} \qquad (10)$$

where:

k_1 and k_i are equilibrium adsorption constants. [S] is the equilibrium concentration of solute. [I] is the concentration of intermediate decomposeition product.

He assumed that the adsorption constants for the decomposition intermediates are the same as those for the original solutes. This assumption was made solely as a simplifying step and without substantiation from independent evidence. Under this assumption, the denominator of equation (10) becomes:

$$1 + k_1[S] + \Sigma k_i[I_i] = 1 + k_1[S]^o \qquad (11)$$

Substitution of expression (11) into (10) gives:

$$\theta_s = \frac{k_1[S]}{1 + k_1[S]^o} \qquad (12)$$

and hence from equation (9)

$$R = k^{11} \frac{k_1[S]}{1 + k_1[S]^o} \qquad (13)$$

He estimated values of R at 50% decomposition, that is, when $[S] = 0.5[S]^o$.

Therefore

$$R = K \frac{k1[S]^{o}}{1 + k1[S]^{o}} \qquad (7)$$

where:

$$K = 0.5k^{11}$$

The data obtained for the rates of oxidation to CO_2 of all 22 solutes were well described by expression (7).

CATALYST

Titanium dioxide is a colorless crystalline solid. It occurs naturally in three crystalline forms: anatase, brookite and rutile. These crystals are substantially pure titanium dioxide but usually contain small amounts of impurities, e.g., iron, chromium, or vanadium, which darken them. Only anatase and rutile are produced commercially, rutile pigments being the largest in volume. Rutile ore contains approximately 95% titanium dioxide. Natural deposits of mineral rutile are rare, being confined mainly to Australia and Africa, and its availability is relatively limited. The only known deposit of anatase ore in the World is the recently discovered anatase ore in Brazil. Chemically pure titanium dioxide is best prepared from titanium tetrachloride (chloride process) that has been purified by repeated distillation (14). The chloride process is currently used to varying degrees by all the major titanium dioxide producers throughout the world.

Titanium dioxide is used extensively in the electronics, plastics, ceramics, inks, rubber, paper, textiles, food and pharmaceuticals industries, but the paint industry is by

far the largest consumer of titanium dioxide pigments. The use of TiO_2 in water treatment processes is rare, because of two reasons: first it is in the research and development stage, and second it is used in minute quantities as catalyst just to promote the rate of dissociation of organic matter.

It is well established that pigmented coatings subjected to weathering undergo oxidative destruction due to incident ultraviolet radiation, in the presence of oxygen and water. Two degradation mechanisms are responsible: direct photochemical degradation by ultraviolet radiation and photoactivity resulting from titanium dioxide. It has been shown (15) that the rate of photochemical degradation is dependent on the following:

1. The energy provided, that is, the wavelength of the incident radiation - the shorter the wavelength the greater the energy.

2. The intensity of the radiation.

3. The absorption characteristics of the solute.

Photocatalytic degradation occurs when ultraviolet radiation absorbed by titanium dioxide causes photochemical reactions, which result in the breakdown of the surrounding

medium. Absorption of a photon by a semi conductor such as, TiO_2 (Fig. 2) excites an electron from the valence band to the conduction band, generating positive holes and free electrons.

$$TiO_2 + h\nu \text{ -------> } e^- + hole^+ \quad (1)$$

The excitation of electrons from valence to conduction band takes place when the photon energy, $h\nu$, equals or exceeds the TiO_2 band gap energy, E_g.

$$E_g = E_c - E_v \quad (2)$$

where:

E_c is the lowest conduction band level energy.

E_v is the higher valence band level energy.

Both the excited electrons and holes are free to move within the crystal lattice of TiO_2, where they may recombine. However, should electrons or holes reach the surface of the titanium dioxide crystal, they are capable of initiating the following series of chemical reactions:

$$TiO_2 + h\nu \text{ -----> } e^- + hole^+ \quad (1)$$

$$hole^+ + OH^- \text{ -----> } OH\cdot \text{ (ads)} \quad (3)$$

$$e^- + O_2 \text{ -----> } O_2^- \text{ (ads)} \quad (4)$$

$$O_2^- \text{ (ads)} + H_2O \text{ -----> } OH^- + HO_2\cdot \quad (5)$$

Both the hydroxy($OH\cdot$) and perhydroxy($HO_2\cdot$) radicals can

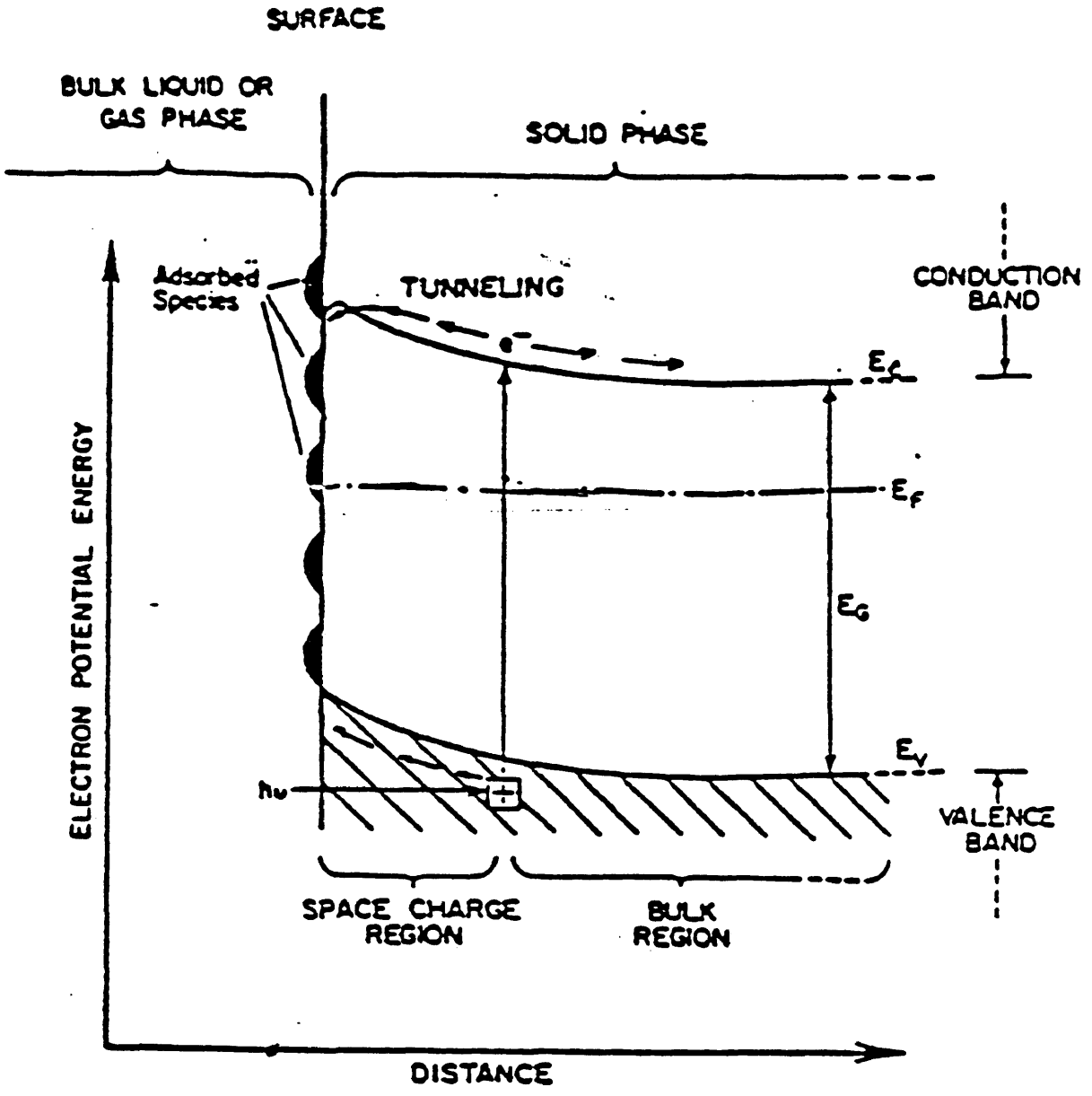

Fig.2: Photoactivation of an n-type semiconductor catalyst (E_C = lowest conduction band level, E_V = highest valence band level, E_F = Fermi level, E_G = band gap of semiconductor (= E_C-E_V). Curved arrows indicate direction of net charge movement at steady state (1,17).

initiate the breakdown of the organic solute. It is evident from the aforementioned reactions that oxygen and moisture are essential for photocatalytic degradation to occur. It has long been known that the anatase form of titanium dioxide is significantly more photoactive than the rutile crystal structure (15).

EXPERIMENTAL TECHNIQUE

Experimental runs for photocatalytic decomposition of Red-79 dye were carried out in three different modes of operation in order to enable me to determine the process viability and make techno-economic assessment of the water decontamination process.

First of all the operation was performed on laboratory scale using an artificial U.V. source, so that I was able to keep a constant flux condition. In the next step bench scale operation was carried out under the actual field conditions, using U.V. rays obtainable directly from the Sun. Finally pilot plant operation was set-up in order to get techno-economic data for photocatalytic decomposition of Red-79 and Blue-80 dyes. Bench scale and pilot plant operations were conducted to correlate the laboratory data.

1.Laboratory scale operation:

The schematic of this mode of operation is shown in Figure 3. An open Pyrex evaporating dish 15 cm. in diameter and 8 cm. deep with flat bottom was used as photocatalytic reactor. Continuous stirring was provided by a VWR magnetic

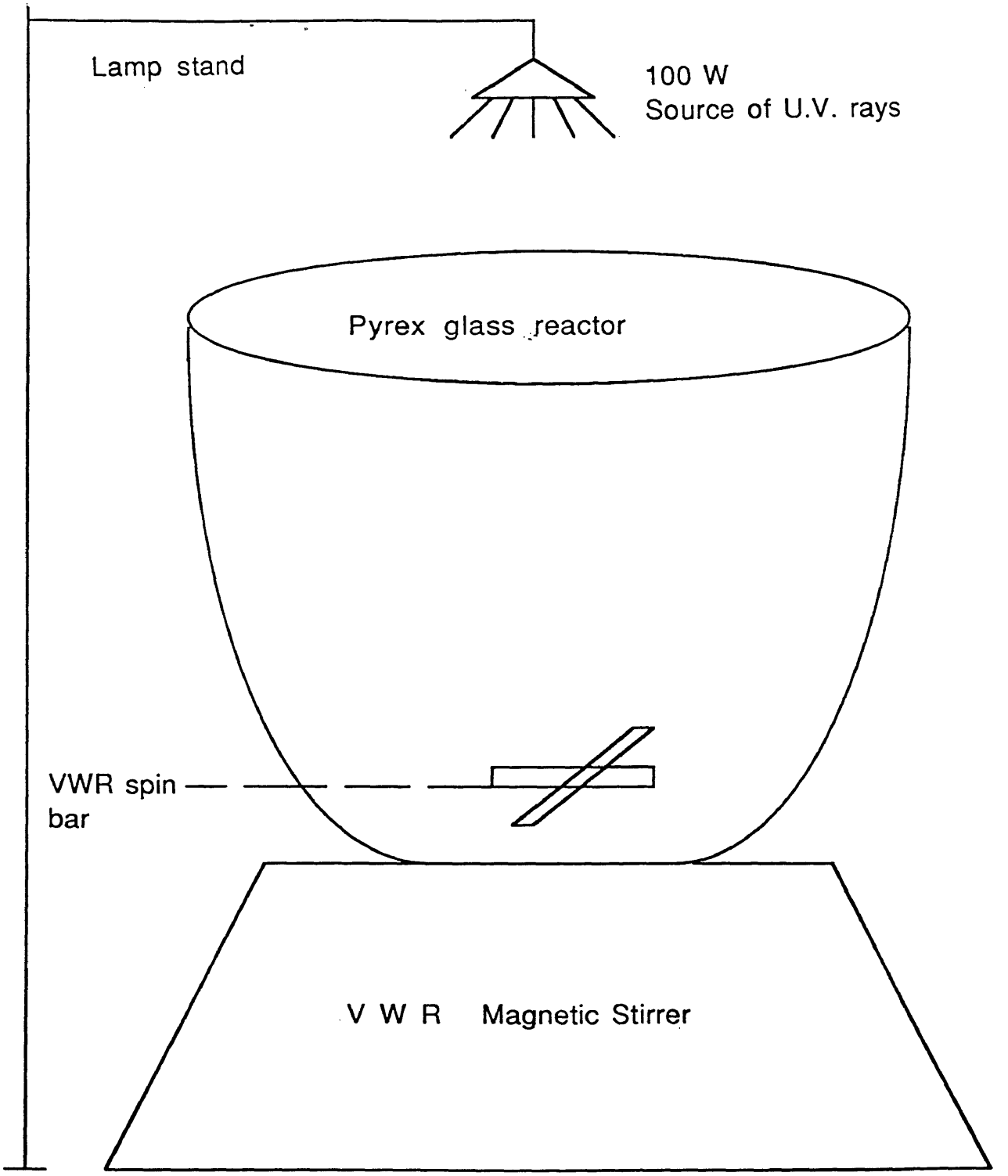

Fig. 3: Schematic of a laboratory scale Red-79 dye photo-decomposition process.

stirrer model-370. One 100-W longwave mercury spot lamp (Blak-Ray longwave U.V. lamp model B-100A) provided illumination. The lamp was oriented in the middle of the reactor and was placed as close as possible to the reactor in order to minimize the scattering of U.V. rays out of the reactor. Outside diameter of the lamp was 12.70 cm. Few experimental runs were carried out under dark room conditions, but no significant reaction effects were observed with either the dark room or ambient room light conditions. The catalyst used in these experiments was Degussa P-25 Titanium dioxide. The crystal structure of the catalyst was anatase and the particles were spherical and non-porous. Its purity was >99.50% TiO_2. The complete specification, as provided by the manufacturer, can be found in Table 3 in the section of comparative process analysis. The powdered semiconductor catalyst was used as supplied, without any pretreatment (thermal or chemical). The Red-79 dye (M.W. = 960 gm/gm-mole, C.I.#29065) used was supplied by M/S Rite color chemical co. inc. (Batch no. 3968). The solution of dye was prepared in de-ionized water. A 200 ml. slurry of Red-79 dye (with varied initial concentrations) and 0.3%w TiO_2 were exposed to U.V. light and the solution was continuously

stirred slowly with the magnetic stirrer. The temperature was noted manually at different time intervals by a laboratory thermometer. The samples were collected in a test tube with a Pasteur pipette. During the initial period of degradation, samples were collected every four minutes, but later on the sampling period was increased to 10-15 minutes, since the degradation rate was high in the beginning. The samples collected from the batch run were left in the dark overnight to settle out most of the TiO_2 particles. The samples were then transferred to disposable centrifuge tubes and were centrifuged in a clinical centrifuge in order to get the maximum possible separation of TiO_2 particles from Red-79 solution. After centrifuging the samples were put in disposable polystyrene cuvettes (Fisher Scientific) and measured in a spectrophotometer (Spectronic-601) for change in concentration. Spectrophotometer readings of absorbances were converted to concentrations (ppm) using characteristic curves for Red-79 and Blue-80 dyes (appendix-B). Figure 4 is a graphical representation of concentration vs illumination time data for one of the experiments, which was performed using techniques described in the aforementioned paragraphs. I studied most of my process variables on laboratory scale.

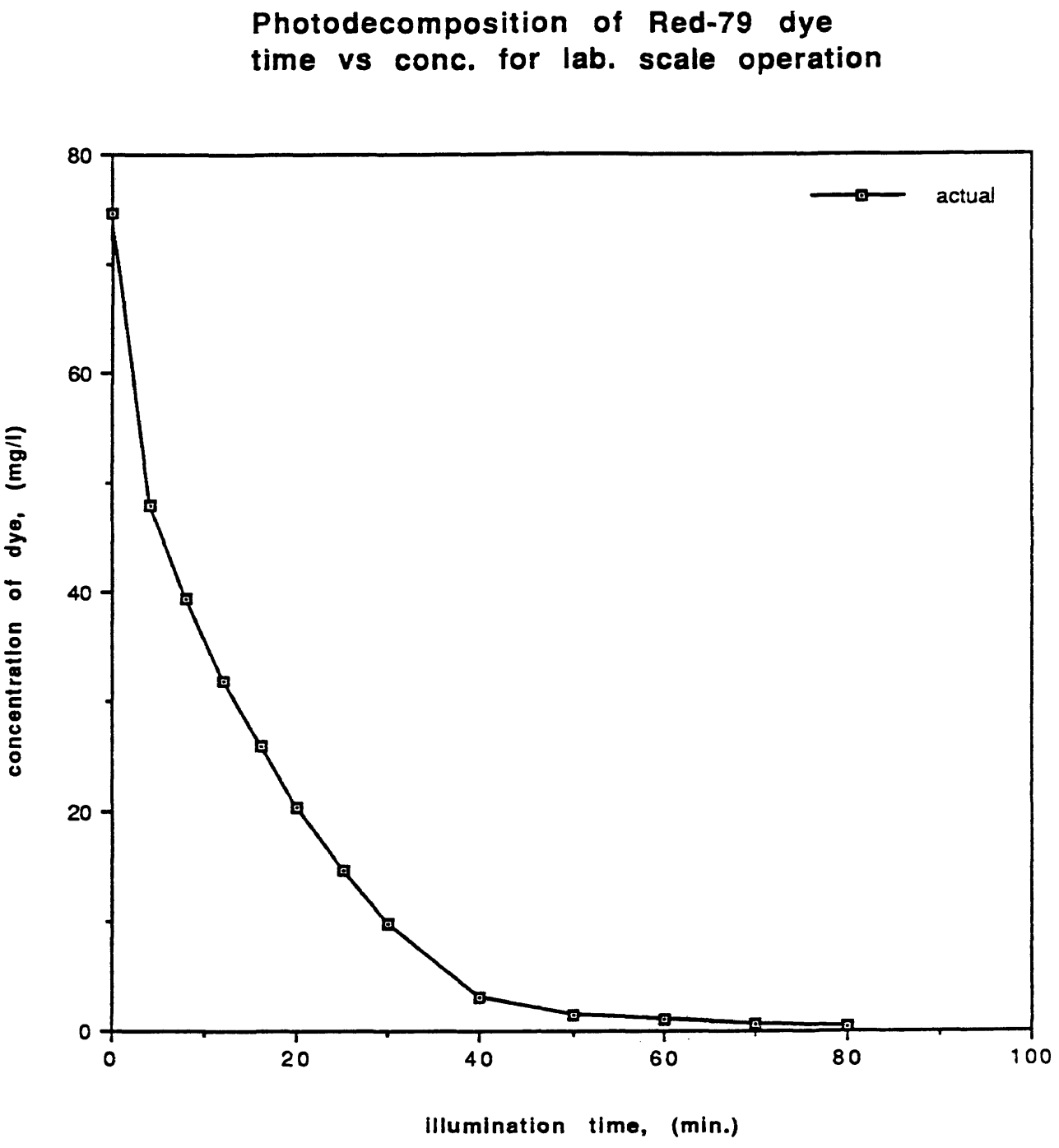

Fig. 4: Graphical representation of illumination time vs concentration data for a laboratory scale experiment. (data source: Table 7, appendix-C).

2.Bench scale operation:

This mode of operation was carried out using U.V. rays from the sun. A Schematic of the process is shown in Fig. 5. These experiments were done in spring'90. Two equal volumes (200 ml.) of Red-79 dye solution were prepared in deionized water. An open glass pan was used as a photoreactor. 0.3%w TiO_2 catalyst, was added to one of the solutions, while the other was free of any catalyst in order to demonstrate the photocatalytic effect of the process. No agitation/stirring was carried out in this mode of operation. Both of the solutions were subjected to solar radiation at the same time. Samples were collected from both of the solutions at different time intervals and were filtered and analyzed in the same way as described in the previous section. Table 1 shows the experimental conditions and results of this one sun experiment. Figure 6 is a graphical representation of time vs concentration data. It is evident from Figure 6 that the dye solution without TiO_2 didn't show any substantial degradation, compared to substantial degradation for the solution with TiO_2, which confirms the photocatalytic effect of the process.

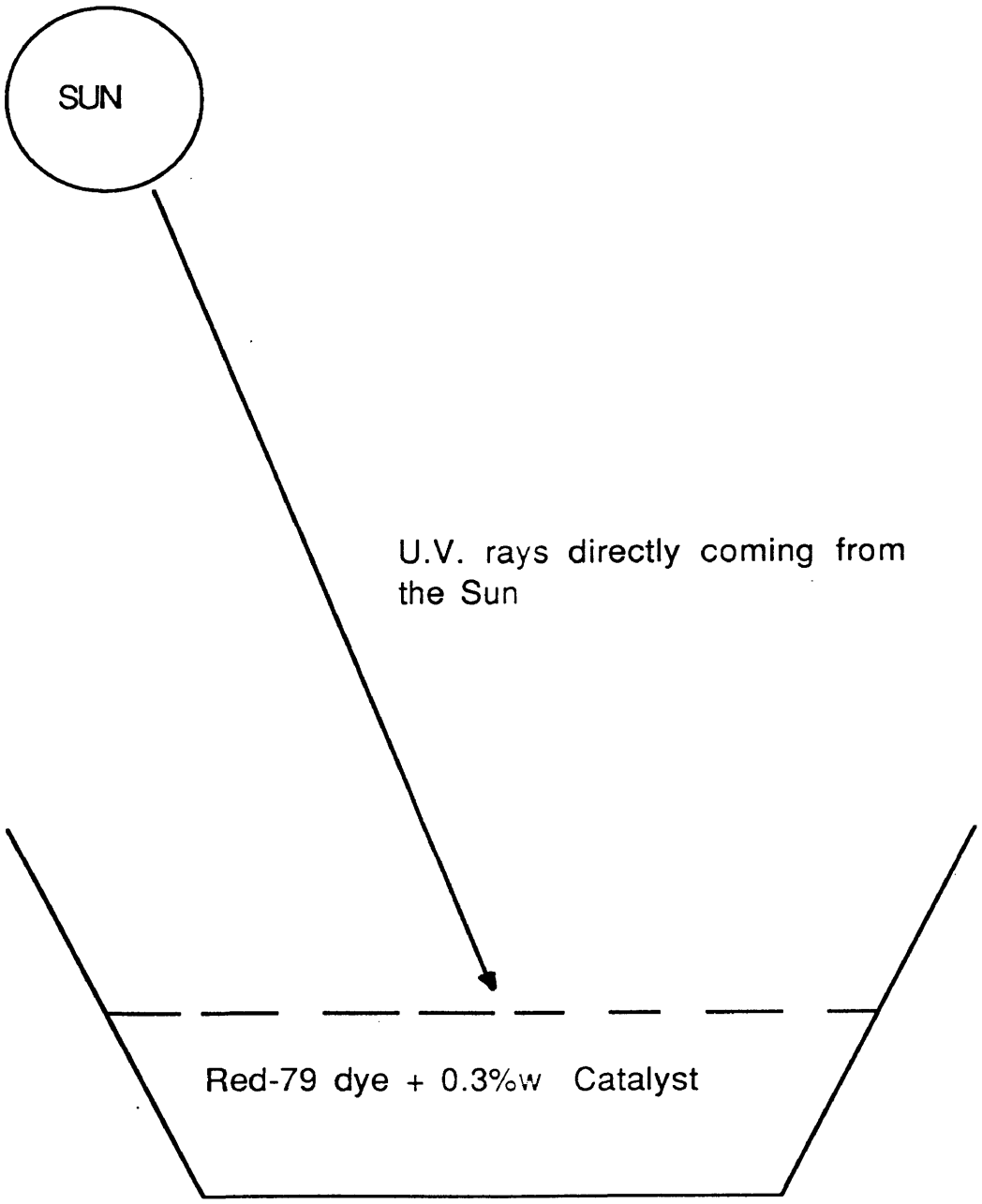

Fig. 5: Schematic of a bench scale Red-79 dye photodecomposition process.

Table. 1: Experimental conditions and results for photodecomposition of Red-79 dye (Bench scale one sun experiment).

Time [hr:min]	Run time [min]	Outdoor condition	Concentration (ppm) dye only	dye+TiO_2
11:00	0	sunny	56.50	50.00
11:10	10	sunny	-	27.85
11:15	15	sunny	56.00	-
11:20	20	sunny	-	17.50
11:30	30	sunny with haze	55.20	12.00
11:45	45	sunny	-	6.50
12:00	60	sunny with haze	53.40	3.00
13:00	120	sunny	-	1.30

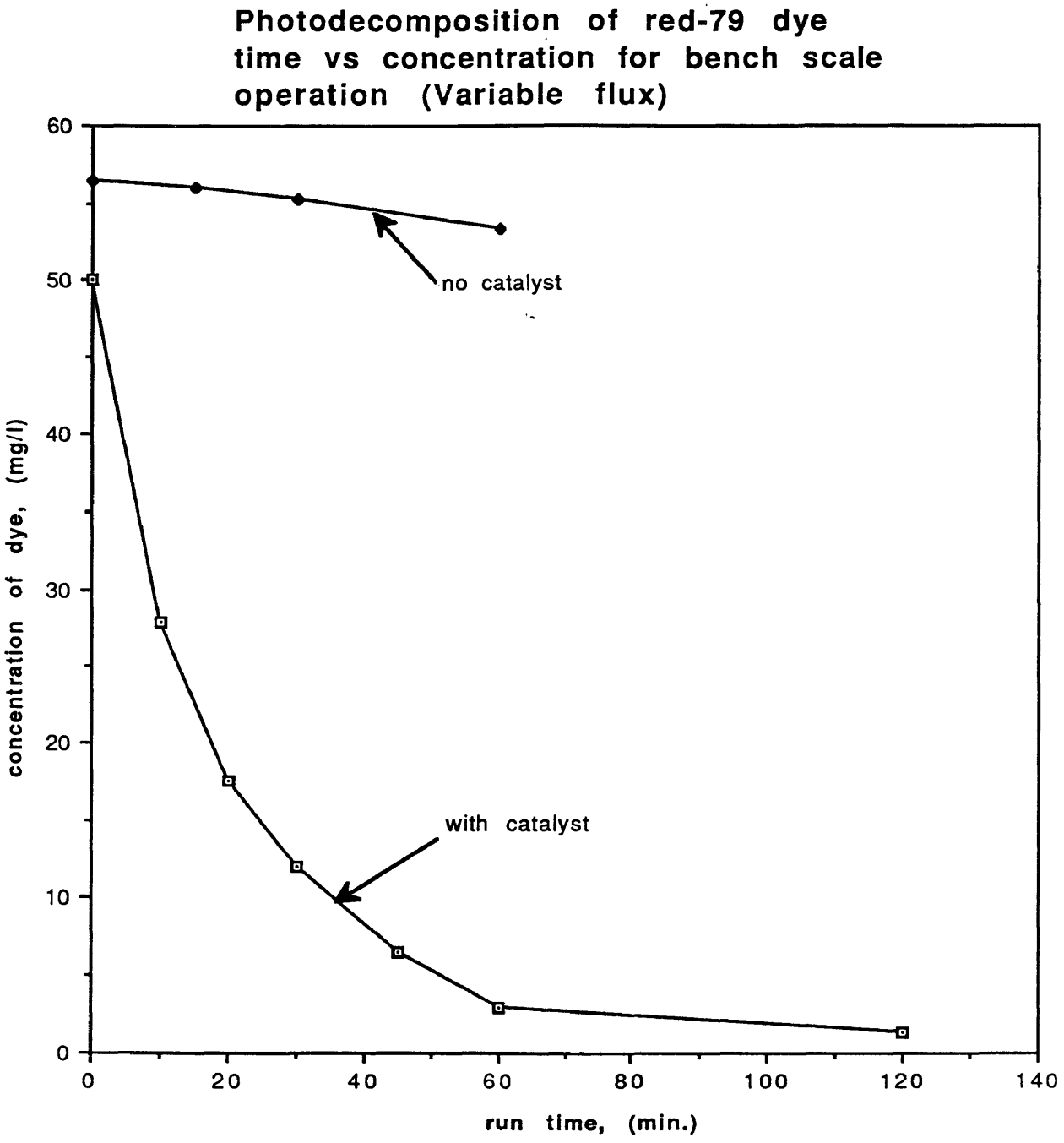

Fig. 6 Graphical representation of run time vs concentration for photodecomposition of Red-79 dye of a bench scale operation. (data source: Table 2).

3. Pilot plant operation:

A pilot plant was chosen to investigate the photocatalytic decomposition of Red-79 and Blue-80 dyes. This pilot plant was designed and installed recently by researchers at the Solar Energy Research Institute (S.E.R.I.) to investigate experimentally the photocatalytic decomposition of various toxic organics, found in water supplies on the EPA's listing of priority pollutants (16). Figure 7 shows the flow diagram of the pilot plant used in our study. Its mode of operation is like a batch recycle reactor.

Prior to the operation of the plant, the system was first water washed and was then flushed with de-ionized water in order to make sure that the system was free from any contaminant or impurity, which could inhibit the rate of photocatalytic decomposition of dye. Solution of dye with de-ionized water was prepared in the storage tank[1]. Catalyst TiO_2 (0.3%w) was added to the prepared solution and the mixer[2] was kept on. The mixing serves two purposes. First it keeps the catalyst particles uniformly suspended in solution and second it facilitates the absorption of oxygen by water. The mixture of catalyst and dye solution was

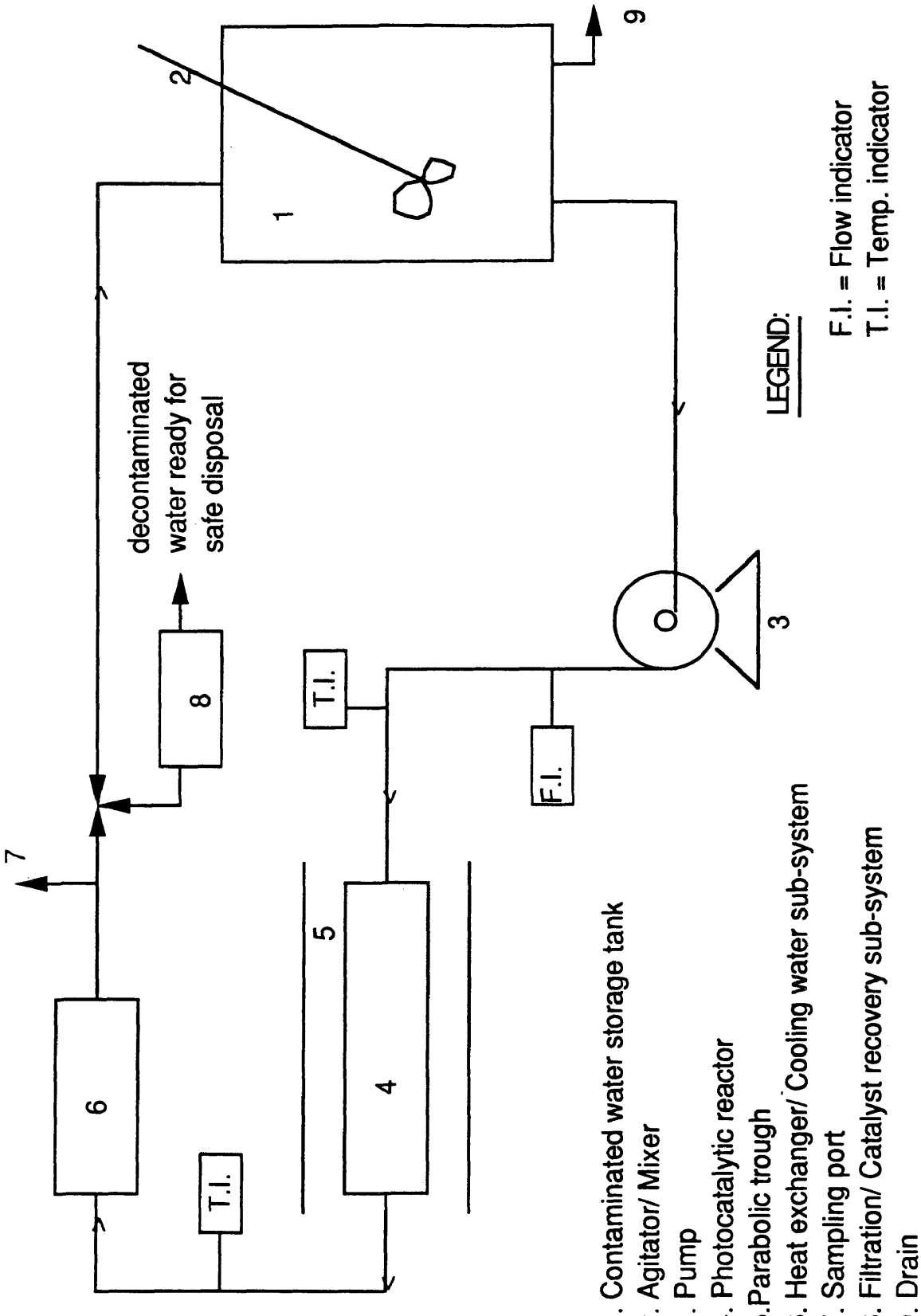

Fig. 7: Flow diagram of a pilot plant for photo-catalytic decomposition of dilute organics.

pumped into a photoreactor [4] from the storage tank by a centrifugal pump [3]. The photoreactor is a transparent borosilicate glass pipe on which a parabolic trough [5] reflects sunlight at a typical radiation level equivalent to 5-10 suns. The dye solution then returns back to the storage tank through a heat exchanger/cooling water system [6]. The samples were drawn periodically through the sample port [7]. Reactor inlet, outlet and ambient temperatures were also noted from a digital read out of thermocouples, and a flow meter reading was recorded at the same time. The catalyst recovery/filtration system [8] was not used in our runs. The contaminated water storage tank[1] can be emptied at any time of operation or can be drained completely for cleaning purposes by opening the drain valve [9]. The samples drawn at different time intervals were analyzed using the same technique as described earlier.

It is interesting to mention here that except for the parabolic trough and photoreactor, which are fixed on a concrete platform, all other equipments are trolley mounted, so that we can put them in a shelter under bad weather conditions. The details of the pilot plant equipment are given as:

i). Main storage tank:

This is a covered cylindrical nalgene tank having a capacity of about 30 gallons. Catalyst and dye solutions are mixed here along with ambient oxygen. Effluents from the reactor are also recycled back to this storage tank.

ii). Mixer/Stirrer:

It is very necessary to keep the catalyst TiO_2 in suspension. This function is best performed by a mixer mounted on the top of the cover of the storage tank. Mixing is accomplished by a variable speed, gear drive stirrer with a 1/15 h.p. fan-cooled electric motor (Tri-R Stir-R model K43). The stirring paddle for the stirrer is a Cole-Parmer model J-4740-5 teflon stirring blade. It also includes a plastic covered 30 inch long steel shaft. This mixer keeps TiO_2 particles in suspension.

iii) Photoreactor:

The photoreactor is made of borosilicate glass, because it transmits near-UV radiation with a transmittance exceeding 85%. It is 1.5 inch in diameter and 16 ft. long. All piping, valves and thermowells were fabricated from non reactive, non catalytic glass to minimize chemical interactions.

iv). Parabolic trough/concentrator:

The parabolic trough reflects sunlight onto the photoreactor, where the water is treated. The reflector is fabricated from polished aluminum. It reflects near-UV radiation with an optical efficiency equal to 70%. Reflector surface area is 37 sq. ft. It is 16 ft. in length and its concentration is about 12 times that of natural sunlight (12 suns). Sun tracking is provided automatically with a controller, 12V DC. The tracking drive device uses a 1/80 h.p induction motor.

v). Pump:

In our initial runs, we used a 1/12 h.p. variable speed centrifugal pump. It was supposed to have a pumping capacity of 6 g.p.m., but experimental runs showed that, it couldn't go beyond 4-5 g.p.m. Sometimes it also lost suction during the operation. This pump was replaced with a new 1/8 h.p. continuous duty centrifugal pump capable of pumping at higher flow rates. We controlled the flow rate by throttling the pump discharge valve according to our process requirement.

vi). Heat exchanger/Cooling water sub-system:

An all glass coiled Corning model HEG/10 liquid-to-liquid heat exchanger was used to cool the process streams. Tap water was used as cooling media. Further details of the equipment can be found in reference(16).

The operating parameters/process variables of this pilot plant operation were logged in the log sheet as shown in appendix-A. Run time vs concentration data are represented graphically in Figure 8 for this type of operation.

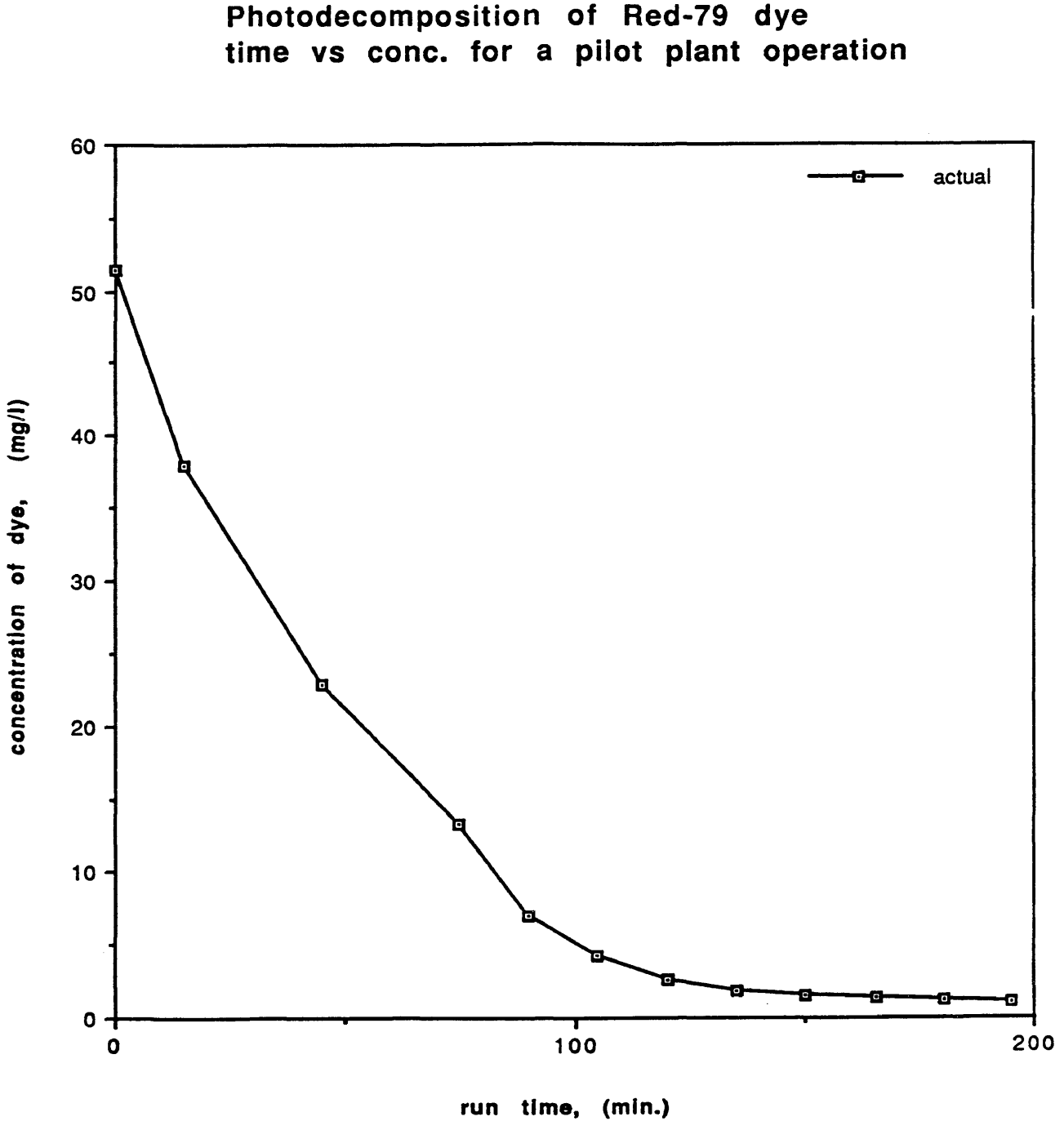

Fig. 8: Graphical representation of run time vs concentration data for a pilot plant operation. (data source: Table 17, appendix-C).

RATE DATA ANALYSIS AND KINETIC MODEL

Differential method of rate analysis:

The reaction for photodecomposition of red-79 dye may be represented as:

$$A \xrightarrow{h\nu + TiO_2} \text{Products} \qquad (1)$$

where A represents red-79 dye.

Here I did not determine the intermediate products and assume that red-79 dye is completely decomposed to carbon dioxide and water. For this irreversible reaction, it is possible to determine reaction order α and the specific reaction rate constant k (18). Assume that the rate law is of the form:

$$-r_a = k(I)\ C_a^{\alpha} \qquad (2)$$

where:

$-r_a$ = rate of decomposition of red-79 dye, mg./l.min.

C_a = concentration of dye at any time t, mg./l.

$k(I)$ = specific reaction rate constant, $(mg./l.)^{1-\alpha}/min$ which is a function of light intensity I.

α = order of the reaction.

Concentration vs time data for one of the laboratory

experiments (Table 7, appendix-C) were differentiated for substitution into equation 2. Sometimes it is preferable to base the rate of decomposition on unit mass of the catalyst. For the experiment of table 7 (appendix-C), I used 0.20 lit. of dye solution and 0.60 gm. of catalyst, i.e., I used 3 gm. of catalyst per lit. of dye solution.

Thus in terms of unit mass of catalyst equation 2 becomes:

$$- r_a' = k'(I)C_a^{\alpha} \text{ ,mg./gm.cat.min.} \qquad (3)$$

where:

$r_a' = r_a/3$ and $k' = k/3$, where 3 gm./l is conc. of cat.

Taking natural logarithm of equation 3, we get:

$$\ln(r_a') = \ln k' + \alpha \ln C_a \qquad (4)$$

A simple linear regression for the data of table 7 (appendix-C) was done using the statistical computer package Minitab release 7 and the following equation was obtained:

$$\ln(r_a') = -3.7614 + 1.0499 \ln C_a \quad (R^2 = 0.929) \qquad (5)$$

from which:

α = order of the reaction = $1.0499 \approx 1.0$

$\ln(k') = -3.7614$ or $k' = 0.02325$ lit./gm.cat.min.

(based on unit mass of catalyst).

$k = 3xk'$ = specific reaction rate constant = 3x0.02325

or $k = 0.06975 \text{ min.}^{-1}$

Substituting value of k just evaluated into equation 2 and the rate equation then becomes:

$$-r_a = (0.06975)C_a \qquad (6)$$

It is important to note that I will use k' throughout my thesis report for the reaction rate constant based on unit mass of the catalyst.

Integral method of rate analysis:

From the differential method of rate analysis, we infer that the order of reaction is 1.0 for the reaction represented by equation 1. The rate equation for a first order constant volume batch reactor is written as:

$$- dC_a/dt = k(I)C_a \qquad (7)$$

Integration of equation 7 gives:

$$\int_{Cao}^{Ca} dC_a/C_a = k(I) \int_{o}^{t} t.dt$$

$$\text{or } \ln(C_{ao}/C_a) = k(I)t \qquad (8)$$

where:

C_{ao} = initial concentration of red-79 dye, mg./lit.

C_a = concentration of dye at time t, mg/lit.

$k(I)$ = specific reaction rate constant, $min.^{-1}$

t = illumination time, min.

The same data, which were used in differential analysis were utilized in equation 8. A plot of $\ln(C_{ao}/C_a)$ vs t gave a straight line with a slope of 0.0706, which is almost the same as that obtained by differential method of rate analysis. The linear plot of rate data by integral method confirmed the order of the reaction, which was determined by the differential method of rate analysis in the previous sec-

tion. It is important to note here that most of the laboratory scale experiments were conducted at constant UV intensity, unless specified.

Development of rate equation for batch recycle reactor:

Batch recycle operation is useful for studying reactions, which are slow (19). The batch operated recycle reactor appears to be particularly well suited for studying the engineering kinetics of slow photo-chemical reactions. Slow photo-reactions are not unusual and may occur when the quantum yield is low (20). Increasing the light intensity improves the rate of slow photo-reactions. However, the increase is limited because of the rather severe restrictions in intensity of available lamps. Moreover we can not control the light intensity during a pilot plant run (actual field conditions). This was one of the basic reasons to select a batch recycle arrangement to study the kinetics of the photocatalytic decomposition of red-79 dye on a pilot plant scale. The schematic of the system is shown in fig. 9.

Doing a mass balance around the entire system of the reactor and reservoir in figure 9. All the connecting lines were wrapped with the aluminum foil in order to make sure that the reaction occurs only in the reactor. The contents of the tank were well mixed by a mixer/agitator, mounted on the top of the tank. Assume that the reactor volume V_r and

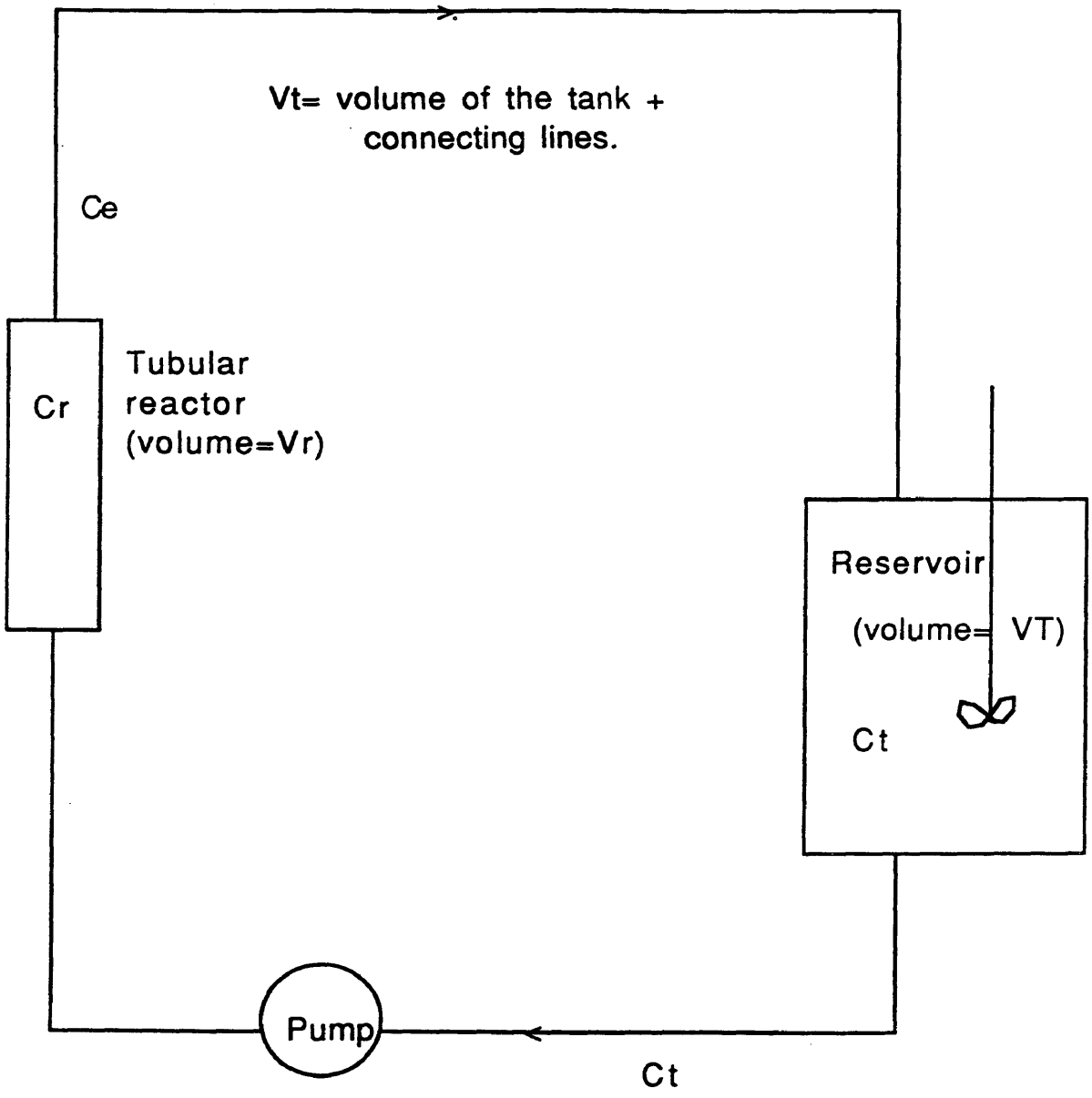

Fig. 9: Schematic of a bath recycle reactor system used in pilot plant experimental runs.

tank volume V_T are constant. Under these conditions, the mass balance equation can be written as:

$$- \int_0^{Vr} r_a dV_r = d/dt[\int C_r dV_r] + V_t dC_t/dt \qquad (9)$$

where:

- r_a = rate of decomposition of red-79 dye.

V_r = volume of the reactor = 1.4688 gals.

C_r = concentration of dye in the reactor.

V_t = volume of the tank + connecting lines = 8.53 gals.

C_t = concentration of dye in the tank.

Since operation was carried out isothermally and the major application of the batch recycle reactor is under conditions of differential reactor operation, therefore, the change in concentration from entrance to exit of the reactor is very small, so that $C_r \approx C_t$. Moreover r_a is nearly constant throughout the reactor for differential operation. Under these restrictions, equation 9 becomes:

$$- r_a V_r = (V_r + V_t) dC_t/dt$$

$$\text{or } - r_a = [(V_r + V_t)/V_r] dC_t/dt \qquad (10)$$

Where r_a is in mg./lit.min. We can also write this equation in terms of unit mass of the catalyst. Equation 10 is the equation for the rate of reaction in a batch recycle reactor, which operates in a differential mode.

In order to check the validity of equation 10, let me do material balance around the reactor only in figure 9.

Let Q be the volumetric flow rate, which was kept constant at about 5 g.p.m., then the mass balance equation around the reactor can be written as:

$$Q.C_t - Q.C_e - \int_o^{Vr} r_a dV_r = d/dt[\int C_r dV_r] \qquad (11)$$

eliminating $d/dt[\int C_r dV_r]$ between equations 9 and 11 gives

$$Q\ (C_t - C_e) = -V_t dC_t/dt)$$

$$\text{or } C_t - C_e = -\ [V_t/Q](dC_t/dt) \qquad (12)$$

Substituting dC_t/dt from equation 10 into equation 12 yields the criterion in terms of operating conditions and the rate of reaction.

$$C_t - C_e = (V_r/Q)[V_t/V_r+V_t]r_a \quad \text{for } (C_t-C_e) \text{ -----> } 0 \qquad (13)$$

Where r_a is the rate of decomposition of red-79 dye. The concentration difference C_t-C_e can be readily calculated for our pilot plant data (table 17, appendix-C) using equ. 13.

$$C_t-C_e = (1.4688/5)(8.5312/10)(6.17145)$$

$$= 1.5466 \text{ mg./lit.}$$

which is a small value compared to 37.9335 mg./lit.; differential reactor operation is approached and equation 9 is valid. The conversion per pass for this change in concentration can be calculated as:

$$(\delta x)_{pass} = [C_t - C_e]/C_t = (1.5466/37.9335) = 0.04$$

$$= 4.0\%.$$

This confirms the validity of using the differential method of rate analysis.

Kinetic Model:

Without going into mechanistic details of kinetic models, we propose two models for which most of the rate data best fit for photocatalytic decomposition of red-79 dye (equation 1). The mechanistic details of phocatalytic decomposition of organic solutes with TiO_2 in the presence of U.V. light have been well represented in the literature (13,21-23). Based on work described in the literature, I have considered both first order and LHHW kinetic models.

Langmuir-Hinshelwood (LHHW) model:

$$r_a = -dC_a/dt = k_1KC_a/(1+KC_a) \qquad (14)$$

Integrating equation 14 from initial concentration of dye C_{ao} to concentration at time t, C_a:

$$\int_o^t dt = -\int_{Cao}^{Ca} dC_a/k_1KC_a - \int_{Cao}^{Ca} dC_a/k_1$$

$$t = (1/k_1K)\ln(C_{ao}/C_a) + (1/k_1)(C_{ao}-C_a) \qquad (15)$$

Where k_1 and K are constants related to the reaction and adsorption properties of the dye.

Now I need to determine kinetic parameters k_1 and K for substitution into equation 15. Method of initial rates can

be used to determine these kinetic parameters.

Equation 14 for the initial rates can be written as:

$$r_{ao} = -dC_{ao}/dt = k_1KC_{ao}/(1+KC_{ao}),\ mg./l.min. \qquad (16)$$

Inverting and rearranging equation 16, which gives:

$$1/r_{ao} = 1/k_1KC_{ao} + 1/k_1 \qquad (17)$$

Data for initial rates were taken from table 19, appendix-C. The linear appearance of plots of reciprocal initial rate vs reciprocal initial concentration can be seen in figure 10. A simple linear regression of equation 17 gave the values of kinetic parameters as follows:

Slope = $1/k_1K = 11.131$; intercept = $1/k_1 = 0.12641$

or $k_1K = 0.08984$,$min.^{-1}$, $k_1 = 7.9108$, mg./lit. min.

and K = 0.0113 lit./mg.

After substitution of the numerical values of these kinetic parameters into equations 14 and 15, those equations become:

$$r_a = -dC_a/dt = 0.08984C_a/(1+0.0113C_a) \qquad (14a)$$

$$t = (11.1311)\ln(C_{ao}/C_a) + (0.12641)(C_{ao}-C_a) \qquad (15a)$$

Now these equations are ready for testing our model at constant U.V. intensity. I will test this model along with the first order model after the development of equation for the first order model.

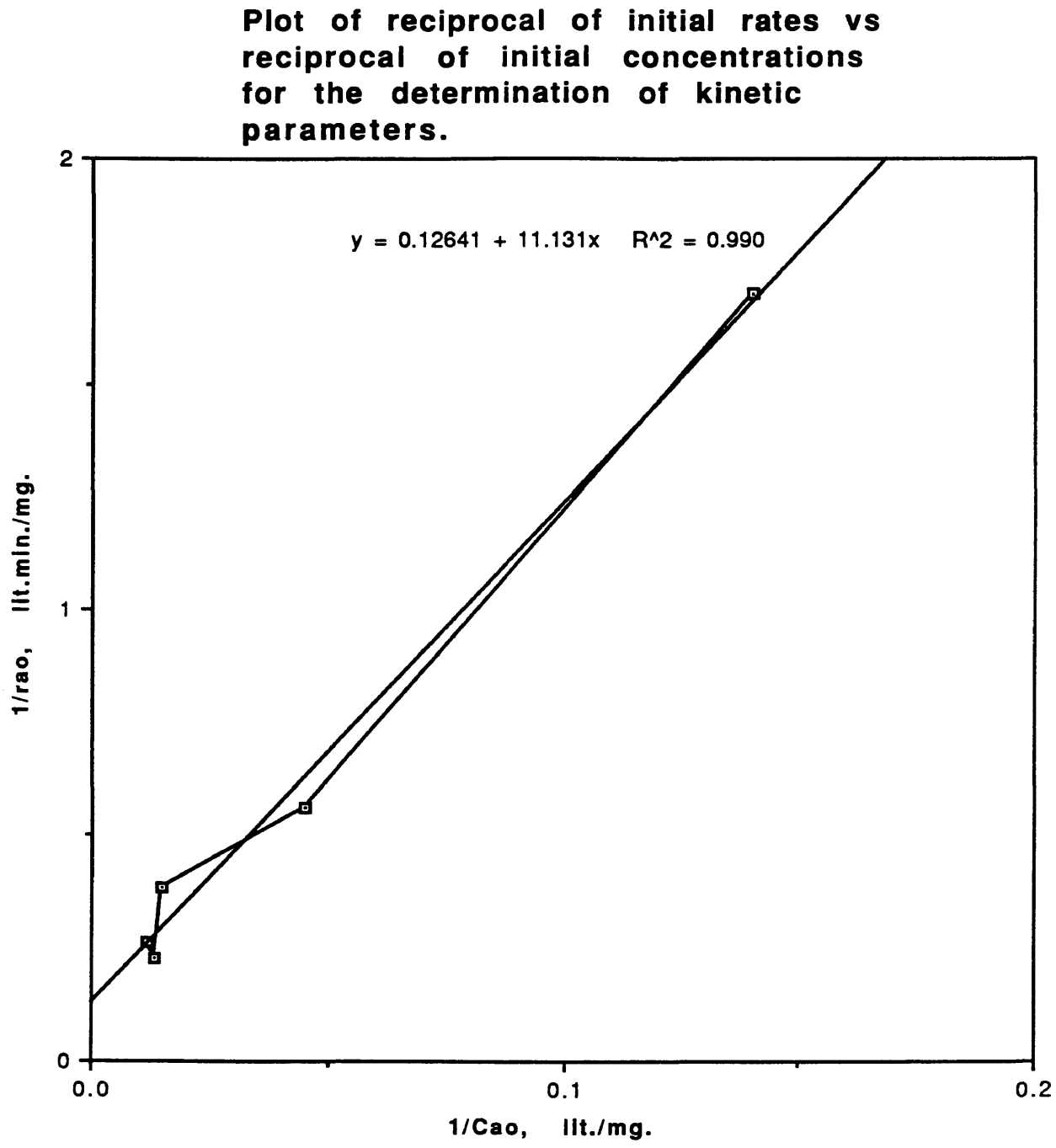

Fig. 10: Initial rate studies. Line is least-squares fit from which kinetic parameters for eqs. 14 and 15 were determined. (data source: Table 19, app.-C).

First Order Model:

$$r_a = -dC_a/dt = kC_a \qquad (18)$$

where:

r_a = rate of decomposition of red-79 dye, mg/lit. min.

k = specific reaction rate constant, $min.^{-1}$

Data of tables 2,3,5 and 7 of appendix-C show that first order rate constant k varies from 0.05 to 0.07, so taking an average value of 0.0616 $min.^{-1}$ for k (for constant U.V. intensity), equation 18 becomes:

$$r_a = -dC_a/dt = (0.0616)C_a \qquad (18a)$$

From equation 18a, we can write:

$$(0.0616)dt = -\, dC_a/C_a$$

Integrating the above equation, which gives:

$$(0.0616)\int_o^t dt = -\int_{Cao}^{Ca} dC_a/C_a$$

$$(0.0616)t = \ln(C_{ao}/C_a)$$

$$\text{or } t = [\ln(C_{ao}/C_a)]/(0.0616) \qquad (19)$$

Equation 19 is now ready for the testing of first order model for constant U.V. intensity.

Model Testing:

$$r_a = 0.08984C_a/(1+0.0113C_a) \qquad (14a)$$

$$r_a = 0.0616C_a \qquad (18a)$$

Let us see, up to what concentration of red-79 dye, the second term in the denominator of equation 14a can be neglected as compared to 1. Having a close look on equations 14a and 18a, I observe that at low concentrations of solutes, equations 14a and 18a are almost the same and the concentration of dye at which the rates evaluated by both of the equations are exactly the same can be calculated by solving equations 14a and 18a simultaneously for C_a. At equal decomposition rates of red-79 dye:

$$0.0616C_a = 0.08984C_a/(1+0.0113C_a)$$

$$\text{or } 0.0616C_a(1+0.0113C_a) = 0.08984C_a$$

$$\text{or } 1 + 0.0113C_a = 1.4584$$

$$\text{or } C_a = 40.57 \text{ mg./lit.}$$

For the experimental data presented in appendix-C, I can neglect the second term in the denominator of equation 14a for initial concentrations of 7.14 ppm and 22.3 ppm, but I can not neglect the second term of the denominator of equation 14a for initial concentrations of 68.17 ppm and

86.19 ppm or higher.

Now equations 15a and 19 can be used to calculate the reaction time to achieve the same concentration by LHHW and first order models respectively. Figures 11 and 12 show a comparison of experimental data with the two proposed models for two different initial concentrations. A summary of the kinetic parameters, which were evaluated and used during the development of equations for the two proposed models and their testing has been given in table 2.

So far, I have based all of my calculations on constant U.V. intensity. But in actual field conditions or pilot plant runs, light intensity is not constant, so we must use such value of k, which is some function of light intensity I. The complete detail of the dependency of k on I is given in the section of comparative process analysis. Here for data analysis and model testing purposes, I will use the value of k, which was determined experimentally from the pilot plant run data.

From experimental data of table 17, appendix-C, the value of k is 0.0221 $min.^{-1}$ The value of K, the equilibrium adsorption constant of red-79 dye remains unaffected with the variation in U.V. intensity. So we can use the same-

Table 2. Kinetic parameters evaluated and used in the two proposed models at constant U.V. intensity.

Kinetic parameters	Value
k_1K, min.$^{-1}$	0.08984
k_1, mg./lit.min.	7.9108
K, lit./mg.	0.0113
k (average), min.$^{-1}$	0.0616
k' (average), lit./gm. cat. min.	0.0205

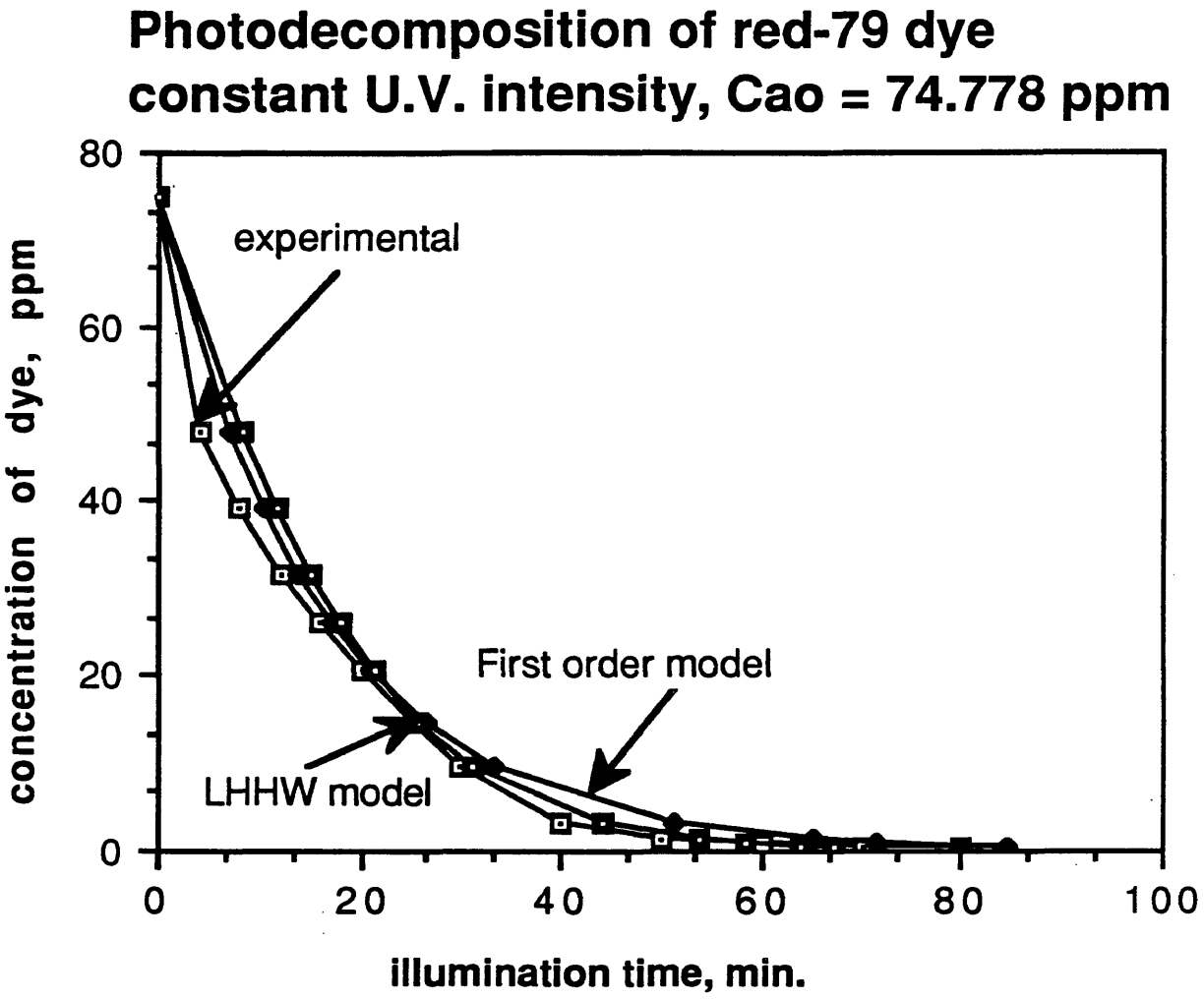

Fig. 11: Comparison of experimental data with the proposed models for a laboratory scale experiment. (Data source: Table 7, appendix-C).

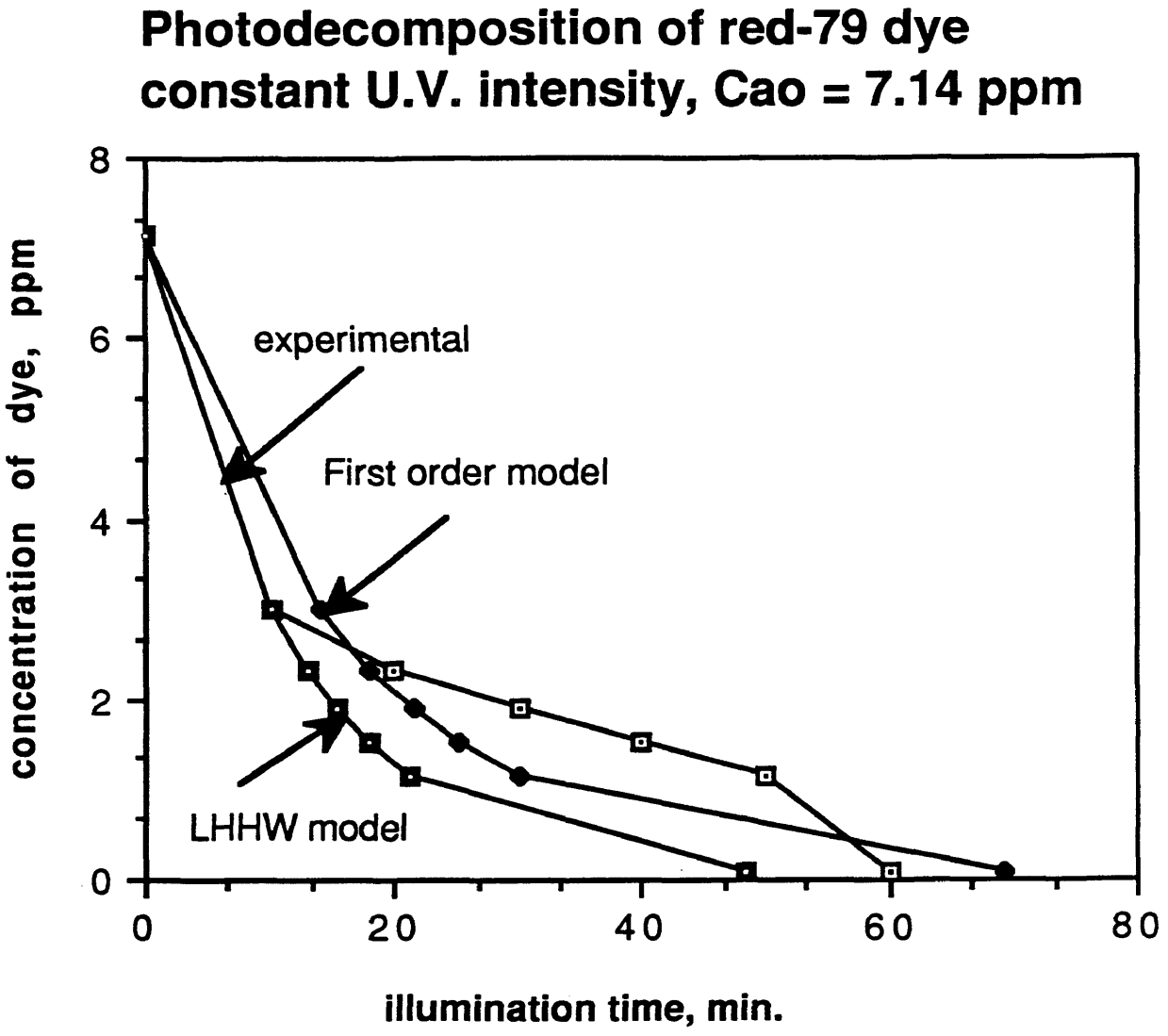

Fig. 12: Comparison of experimental data with the proposed models for a laboratory scale experiment. (Data source: Table 3, appendix-C).

value of K from table 2, which was previously used in the model testing for constant U.V. intensity. Thus using k = 0.0221 $min.^{-1}$ and K = 0.0113 lit./mg., the rate equations for LHHW and first order models become:

$$r_a = - dC_a/dt = 0.0221C_a/(1+0.0113C_a) \quad (20)$$

$$r_a = - dC_a/dt = 0.0221C_a \quad (21)$$

The integrated forms of equations 20 and 21 can be written as:

$$t = (45.25)\ln(C_{ao}/C_a) + 0.1264(C_{ao}-C_a) \quad (20a)$$

$$t = [\ln(C_{ao}/C_a)]/(0.0221) \quad (21a)$$

Equations 20a and 21a are now ready for the testing of two proposed models for pilot plant runs, where U.V. intensity is not constant. The two models have been compared with the experimental data of table 17, appendix-C (pilot plant run) in figure 13.

Thus I conclude that at low concentration of red-79 dye, the rate of photodecomposition of red-79 dye follows a simple first order behavior, while at higher concentration of dye, it follows Langmuir-Hinshelwood kinetics. This conclusion will be further strengthened in the section of comparative process analysis, when I will study the effect of initial concentration of red-79 dye.

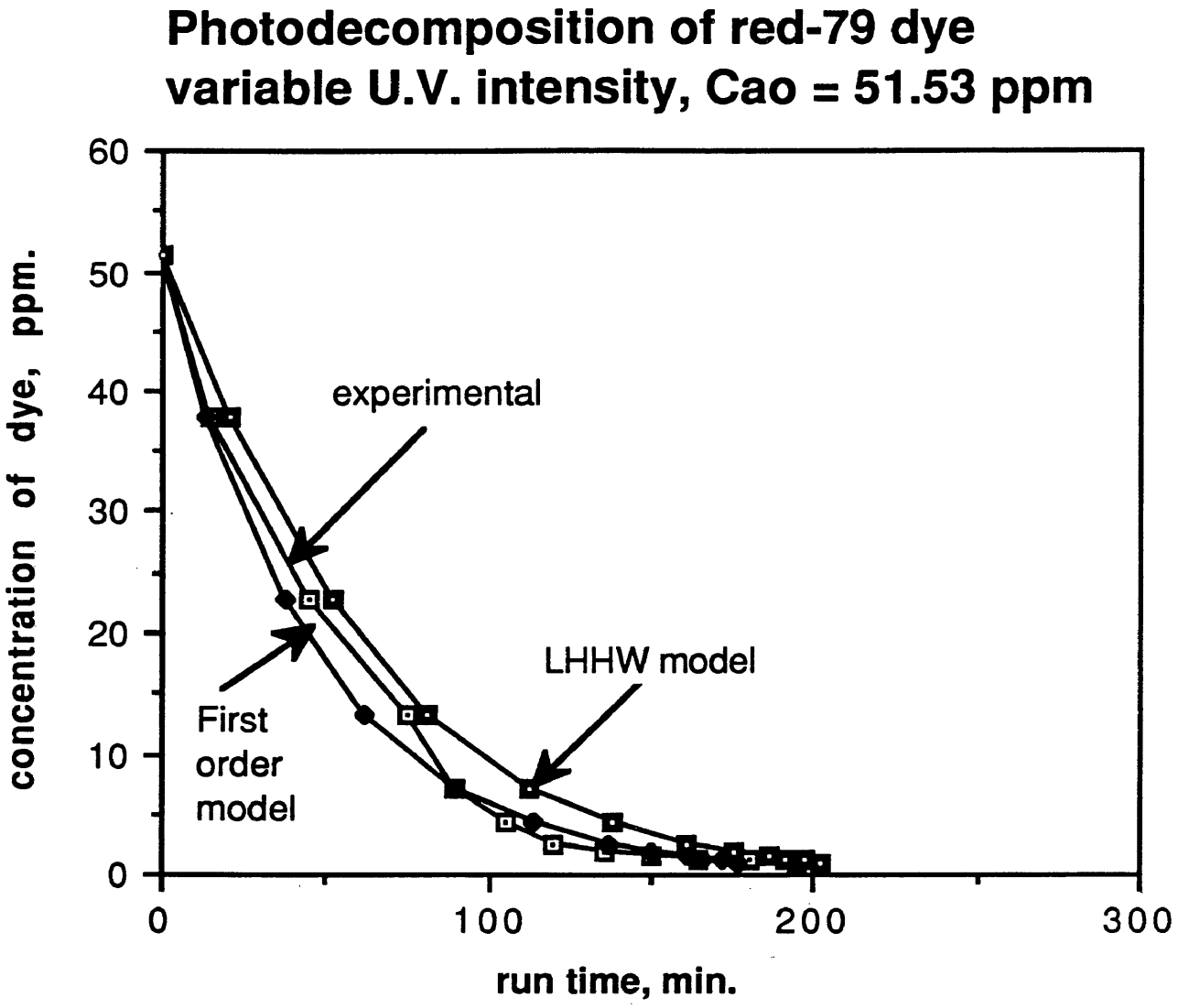

Fig. 13: Comparison of experimental data with the proposed models for a pilot plant experiment. (Data source: Table 17, appendix-C).

COMPARATIVE PROCESS ANALYSIS

Effects of changing process variables:

In this section we will see how the changes in process variables affect the process of photocatalytic decomposition.

i). Catalyst loading:

Catalyst loading is a function of reactor geometry (22). We determined the most effective catalyst loading for our laboratory scale reactor. Figure 14 compares decomposition rates of red-79 dye with 0.1%w, 0.2%w and 0.3%w TiO_2 with almost the same initial concentrations. The experiment for 0.3%w catalyst was performed by the author, while the data for 0.1%w and 0.2%w were taken from the experiments performed in S.E.R.I.'s laboratory under the same operating conditions. The effect of catalyst loading on the first order rate constant (k) is compared in figure 15. The most effective catalyst loading for bench scale operation under one sun condition for red-79 dye was determined by Baltz, P.

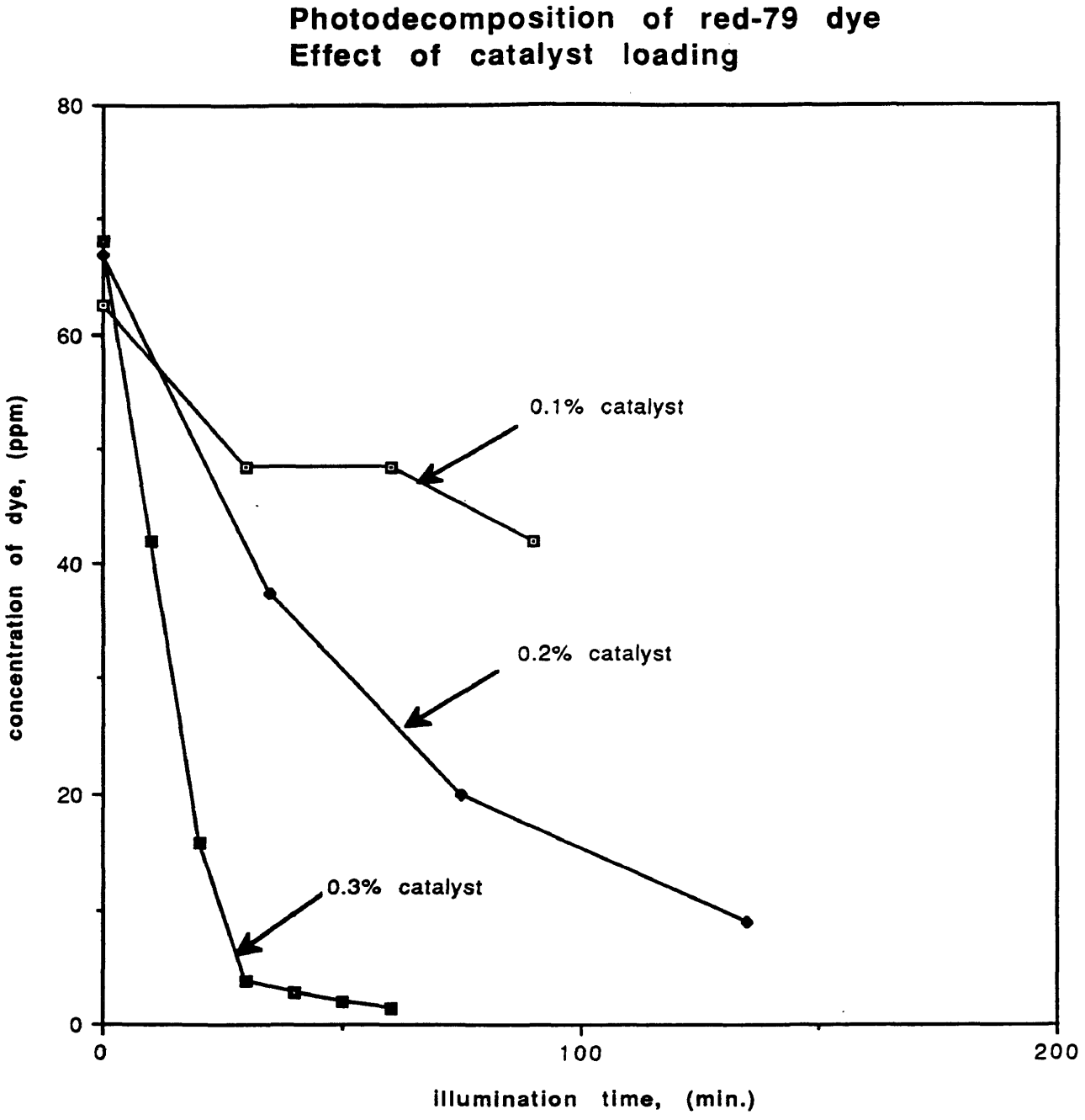

Fig. 14: Effect of catalyst loading on photodecomposition rates of red-79 dye. (Data source: Table 1, appendix-D).

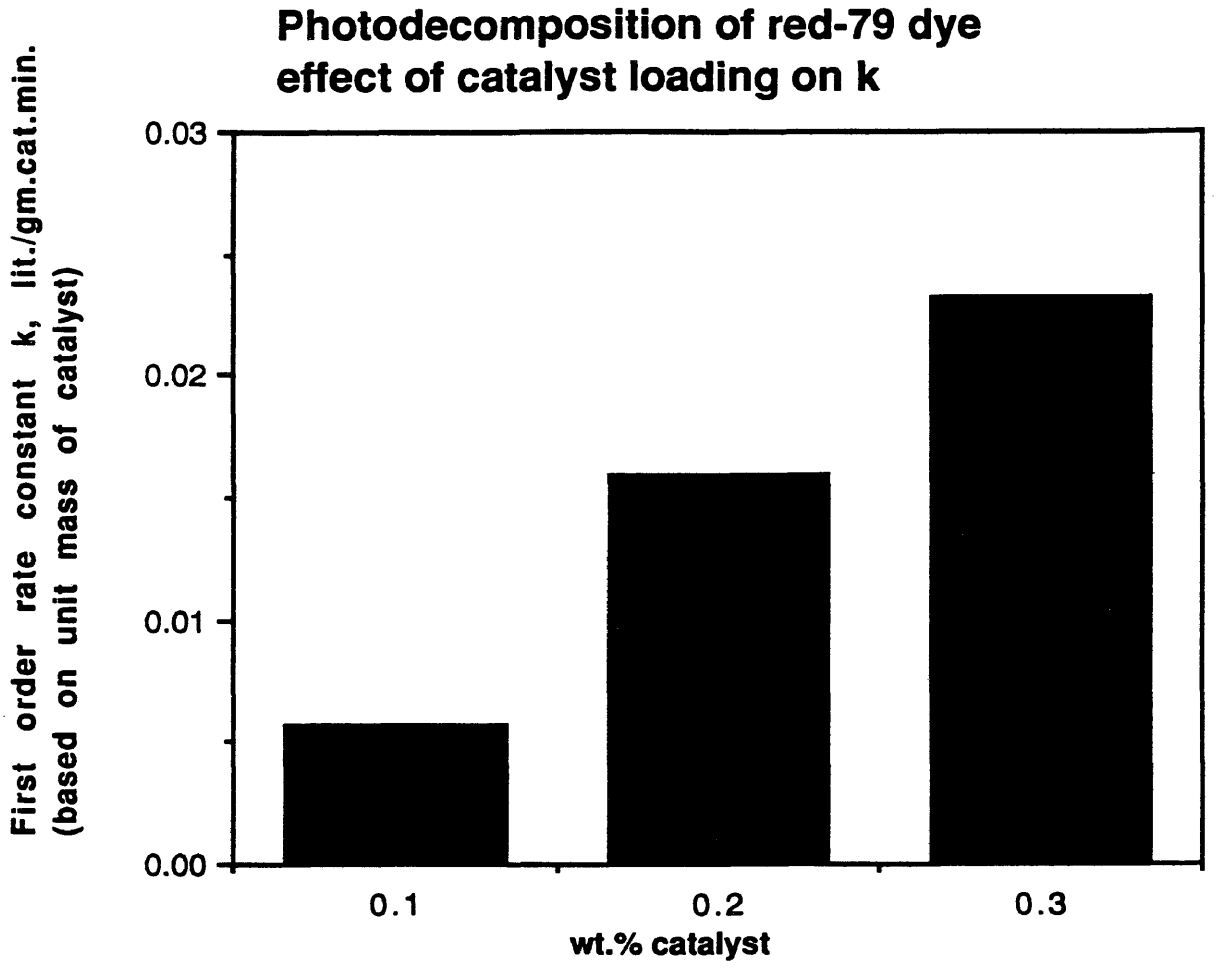

Fig. 15: Effect of catalyst loading on first order rate constant k for photodecomposition of red-79 dye. (Data source: Table 1, appendix-D).

and Meir, B. (24) and was found to be 0.004 weight fraction for variable U.V. intensity.

ii). Effect of impurities on the photoactivity of TiO_2:

Purity of TiO_2 catalyst is very important from the view point of its activity as photocatalyst. Anatase TiO_2 generally has titanium dioxide content, between 95 and 99%, with silica and alumina predominating as coating oxides. A comparison of TiO_2 properties available from three different suppliers is given in table 3.

The addition of small amounts of impurities like SiO_2 and Al_2O_3 can reduce the photoactivity of TiO_2 to one half that of uncoated TiO_2. In order to see the effects of impurities on the activity of TiO_2, two separate runs of experiments were performed in a batch recycle reactor (pilot plant) on two different days. We used red-79 dye as organic solute. Here our objective is just to compare the rates of dissociation of organic solute in the presence of 0.1%w and 0.2%w TiO_2, which is 98% pure. If we go through table 4, we see that TiO_2 provided by M/S Degussa Corporation and Fisher are 99.5% pure, while that by E.M.Science is 98% pure. We

Table 3. Comparison of TiO_2 (catalyst) properties supplied by three manufacturers.

Property/Manufacturer	EM Science	Degussa Corporation	Fisher
i). Purity, %	98.00	>99.50	>99.50
ii). Av. particle size, nm.	N.A.	30	30
iii). sp. surface area, sq.m/g.	N.A.	50±15	7
iv). Formula wt.	79.90	79.90	79.90
v). Density, g/c.c.	N.A.	0.15	3.90
vi). M.P.. ^{o}C	181	N.A.	N.A.
vii). Test method	ACS	ASTM D1208	ASTM
viii). Impurities:			
Al_2O_3	N.A.	<0.30%	N.A.
SiO_2	N.A.	<0.20%	N.A.
water soluble substances	0.30% max.	N.A.	0.15% max.
Arsenic	2 ppm	N.A.	0.0002%
Pb	0.002%	N.A.	0.008%
Zn	0.01%	N.A.	0.01%
Fe	0.01%	0.01%	0.01%
Loss on ignition	0.30%	<0.20%	N.A.
ix). Price, $/500g.	14.85	samples f.o.c.	20.70

N.A. = not available
f.o.c. free of cost
Source: Manufacturers' catalogs.

selected the TiO_2 provided by E.M. Science, which is 98% pure and is believed to contain SiO_2 and Al_2O_3 as impurities. The first experiment was conducted on 04.06.1989 using 0.1%w catalyst, while the other was done on 07.18.89 using 0.2%w catalyst. Tables 4 and 5 present the experimental conditions and results of experiments performed on the above mentioned dates respectively. It is evident from tables 4 and 5 that when we doubled the amount of TiO_2, i.e., when we used 0.2%w TiO_2 instead of 0.1%w, the rate of dissociation of red-79 dye became almost half although the weather conditions were more favorable on that day. Figure 16 compares both experiments.

From the above discussion, it is now clear that we must use high purity TiO_2 in order to promote the rate of detoxification of organic solutes. Thus we discarded the TiO_2 supplied by EM Science and used TiO_2 supplied by M/S Degussa Corporation, which was 99.5% pure in the rest of our experiments.

Table 4. Experimental conditions and results using 0.1%w of an impure TiO_2 catalyst.

Time [hr:min]	Run Time [min]	Temp. [°C]	Outdoor condition	Abs.	ppm
12:00	0	27	sunny	2.342	92.36
13:00	60	29	cloudy	1.810	71.57
13:30	90	33	partly sunny	1.728	68.37
14:00	120	37	partly sunny	1.683	66.61
14:30	150	39	partly sunny	1.676	66.33
15:00	180	41	partly cloudy	1.644	65.09
15:30	210	38	partly cloudy	1.589	62.94
16:00	240	36	cloudy	1.583	62.70

Table 5. Experimental conditions and results using 0.2%w of an impure TiO_2 catalyst.

Time [hr:min]	Run Time [min]	Temp. [^{o}C]	Outdoor condition	Abs.	ppm
11:00	0	30	sunny with haze	1.932	76.34
11:30	30	35	sunny	1.868	73.84
12:00	60	38	sunny	1.811	71.61
12:30	90	42	sunny	1.757	69.50
13:00	120	40	sunny	1.720	68.05
13:30	150	40	sunny	1.698	67.20
14:00	180	39	sunny	1.646	65.17
14:30	210	37	sunny	1.629	64.50
15:30	270	30	sunny with haze	1.606	63.60
16:00	300	30	sunny	1.593	63.09

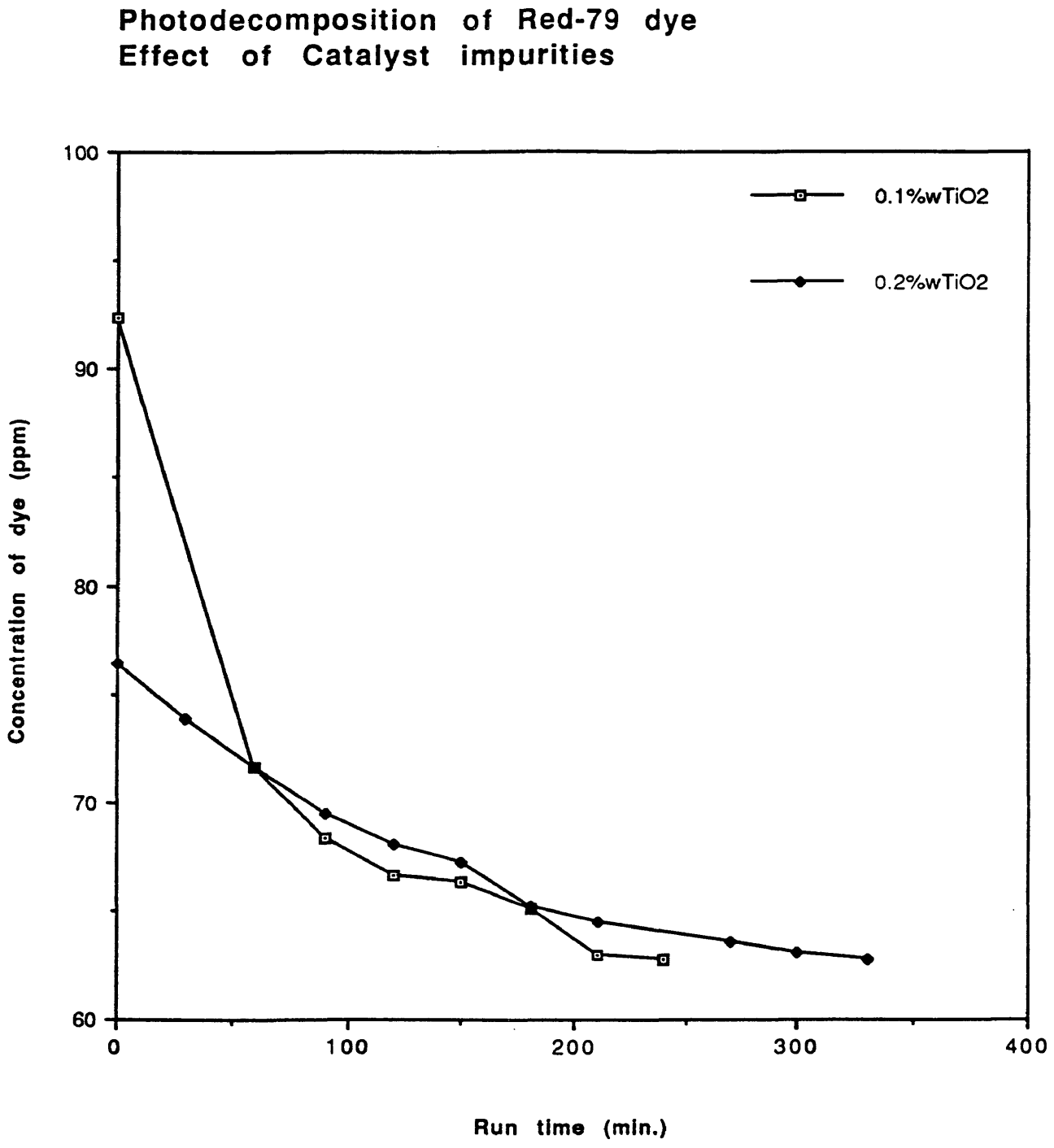

Fig. 16: Comparison of dissociation rates of red-79 dye using 0.1% and 0.2% TiO_2 for 98% pure catalyst. (Data source: Tables 4 and 5).

iii). Addition of hydrogen peroxide (H_2O_2):

To determine the effect of adding hydrogen peroxide three separate runs were made on laboratory scale with almost the same initial concentration. In the first run 200 ml. of red-79 dye solution (Co=76ppm) was dosed with 4 ml. of 30% hydrogen peroxide and were placed under UV lamp in the Pyrex glass reactor. The solutions were stirred slowly by the magnetic stirrer, while being irradiated by UV light. The second run (Co=76ppm) was done under the same operating conditions except that 0.3%w TiO_2 was also added along with hydrogen peroxide. In the third run no hydrogen peroxide was added and 74 ppm initial concentration of red-79 dye solution was irradiated with U.V. light in the presence of 0.3%w catalyst. The results of all these three runs were compared and shown in figure 17. From figure 17, it appears that hydrogen peroxide plays no positive role in improving the kinetics of photodecomposition of red-79 dye. Addition of hydrogen peroxide alone doesn't have any improving effects, but the addition of small amounts of hydrogen peroxide along with the catalyst has been observed (25). The results shown in figure 17 can be explained in the light of Peterson

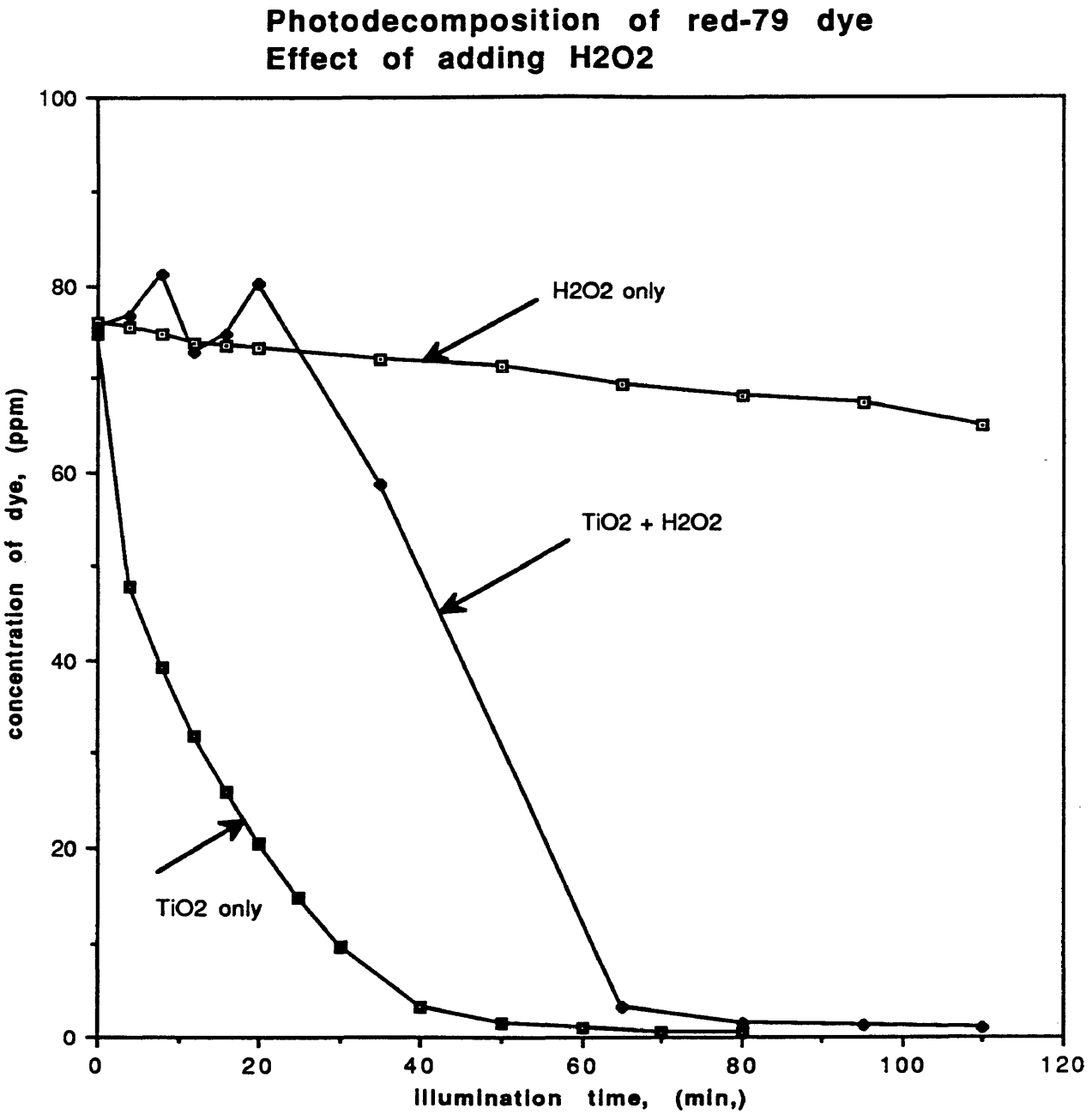

Fig. 17: Effect of adding hydrogen peroxide.
(Data source: Table 7,10 and 11 of appendix-C).

et. al.'s report (25). According to their conclusion, the addition of excess amounts of hydrogen peroxide can decrease the decomposition rate if the concentration of the hydrogen peroxide is sufficiently high.

iv). Variation of U.V. intensity:

A series of four experimental runs were carried out to observe the effect of light intensity on the photodecomposition of red-79 dye. In all of the runs, the same mass of the catalyst was used, 0.3%w, while the initial concentration of the reactant ranged from 65 ppm to 72 ppm. Each run spanned a period of about 2 hours. In the first run, 200 ml. of dye solution containing 0.3%w TiO_2 was put under U.V. lamp from which U.V. rays were coming through a filter (wire gauze with 0.47 transmittance). In the second, third and fourth runs all the operating conditions were same except that instead of one, we put two, three and four filters respectively, each having the same absorbance for overall absorbances of 0.72, 0.85, and 0.92. Since the reactor was placed very close to the U.V. source, we assume that all of the light transmitted is absorbed by the catalyst TiO_2.

The intensity profile of a photon source in an absorbing medium is governed by the logarithmic decrement law known also as Beer's law or Bouguer's law (26):

$$I = I_o \exp(-\text{absorbance}) \qquad (1)$$

where I_o is the incident intensity and was determined by standard actinometric method in SERI's laboratory by Craig S.Turchi. According to him, the rate of photons entering per unit area of the reactor was 6.32×10^{20} photons/m^2sec. There are 5.43×10^{-19} joules in one photon (at 320 nm wavelength) and 1 joule/sec. in 1 watt, therefore:

$$I_o = 343.176 \text{ w/m}^2.$$

The following models were tested for the effect of variation in U.V. intensity on first order rate constant k:

$$\text{Model 1: } k(I) = xI + c$$

$$\text{Model 2: } k(I) = x\, I_c$$

$$\text{Model 3: } k(I) = x \exp(YI) I_c$$

$$\text{Model 4: } k(I) = x\, (I)^{\frac{1}{2}} - c$$

where x, Y and c are statistical constants.

A non-linear regression was done using Minitab and it was found that model-4 best fits our experimental data.

The square root relationship of U.V. intensity I with first order rate constant k (model-4) best fits statistical-

ly, as well as, it provides physical interpretation for photocatalytic decomposition of red-79 dye.

As we have seen earlier in the section of Catalyst (fig.2) that the primary photochemical act occurs inside the TiO_2 crystal. Absorption of photons by TiO_2 excites electrons from the valence band to the conduction band, leaving positive holes in the valence band,

$$TiO_2 + h\nu \text{ -----> } e + \text{hole} \qquad (2)$$

Both electrons and holes are free to move about the crystal lattice and in doing so, they either recombine or reach the surface, where they can initiate chemical reactions in the surrounding medium. The relative magnitudes of the recombination and surface reaction rate constants then determine the dependence on light intensity of the overall reaction rate (27). Although, I have already presented a brief mechanism for the formation of hydroxy($OH^{\cdot}$) and perhydroxy ($H2O^{\cdot}$) radicals from literature, however, it will be interesting to recall them here:

$$\text{hole} + OH^- \text{ ------> } OH^{\cdot} \text{ (ads.)} \qquad (3)$$

$$e + O_2 \text{ -------> } O_2^- \text{ (ads.)} \qquad (4a)$$

$$O_2^- \text{ (ads.)} + H_2O \text{ ------> } OH^- + HO_2^{\cdot} \text{ (ads.)} \qquad (4b)$$

Either the hydroxy, $OH^{\cdot}$, or perhydroxy, $HO_2^{\cdot}$, radical may

initiate breakdown of the organic dye.

The rate dependency on I was studied by Egerton and King (27) and it was found that under the light intensities normally encountered, the rate was proportional to the square root of the light intensity. This conclusion was shown to be a consequence of the processes occurring in the TiO_2 crystal, when illuminated by U.V. light. According to them (Egerton and King), the final rate equation thus obtained is:

$$-r_a = K(I)^{\frac{1}{2}} \qquad (5)$$

Equation 5 supports my proposed model. The constant c in my proposed model is some sort of threshold or effective intensity of sunlight, below which the reaction is not possible.

The square root dependency of my experimental data along with the proposed model is shown in figure 18. Some other researchers have also found the same dependency of k on I for photocatalytic decomposition of organic solutes in the presence of TiO_2 catalyst (3,25).

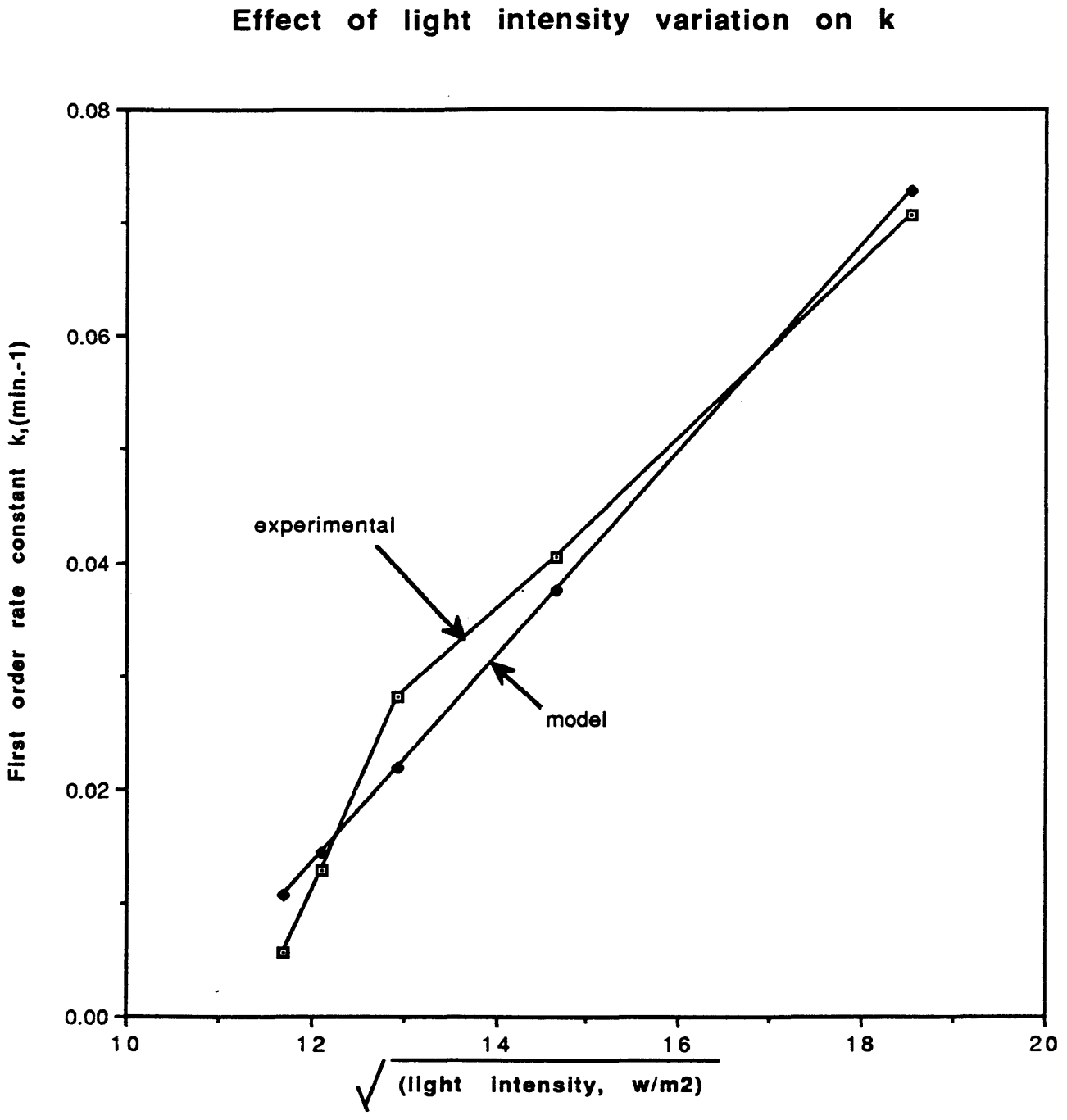

Fig. 18: Effect of light intensity on the photodecomposition of red-79 dye. (Data source: Table 2, appendix-D).

v). Effect of temperature:

The temperature rise of about 10°C took place in the first hour of operation (laboratory scale at constant U.V. intensity), then it became almost constant. In the pilot plant experiment, the temperature was controlled through a heat exchanger and no measurable temperature gradient existed. No distinguishing effect of temperature was also observed on reaction rate constant k by the researchers at Solar Energy Research Institute at constant U.V. intensity. This is because the rate limiting step is thought to be absorption of photon to form a free electron and a positively charged hole. Thus the reaction sequence is photoinitiated rather thermally initiated.

vi). Effect of initial concentration:

In order to observe the effect of initial concentration, some experimental runs were conducted with different initial concentrations of solute (red-79 dye) keeping light intensity and mass of the catalyst as constant. The effect of initial concentration of red-79 dye on the rate of photo-

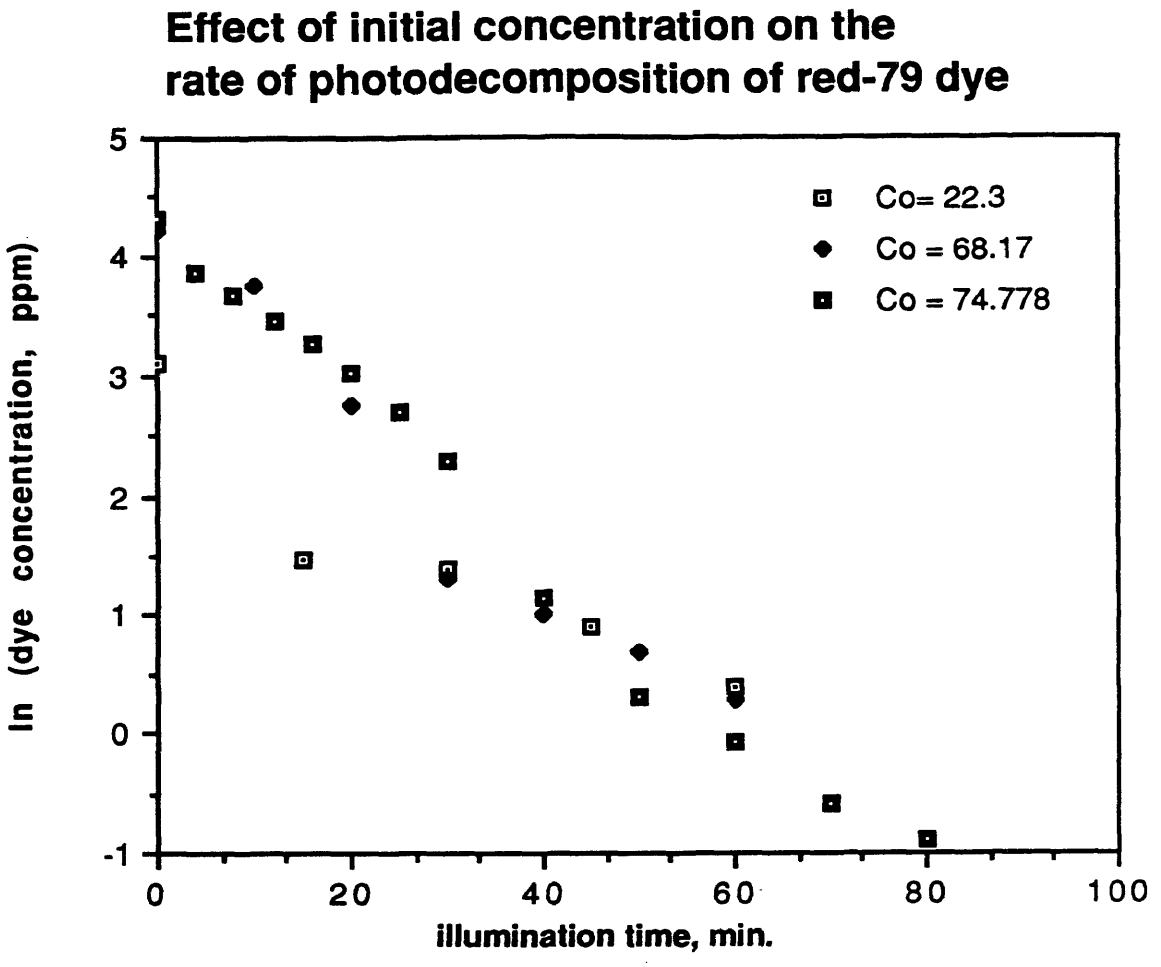

Fig. 19: Effect of initial concentration of red-79 dye on the rate of photo-decomposition. (Data source: Tables 2, 5 and 7, appendix-C).

decomposition of dye is shown in figure 19. From figure 19, it can be seen that there is an approximately linear decrease in the logarithm of the dye concentration with illumination time.

The expression

$$\ln(C_{ao}/C_a) = kt$$

is a good approximation over the concentration as low as 22.3 ppm or as high as 74.778 ppm. The following table presents the values of specific reaction rate constant k for different initial concentrations.

Specific reaction rate constant, k for different initial concentration of red-79 dye, C_{ao}:

C_{ao}, ppm	k, $min.^{-1}$
7.14	0.053
22.30	0.050
68.17	0.073
74.78	0.071
86.19	0.044

From above, it is clear that the first order rate constant k remains almost constant at low concentration of dye, i.e., 7.14 ppm and 22.3 ppm, but it decreases with the

increase in dye concentration at higher concentration of red-79 dye, i.e., 68.17 ppm, 74.778 ppm and 86.19 ppm. This observation strongly supports my conclusion for proposed models in the section of kinetic models.

vii) Catalyst deactivation:

Two experiments were carried out to investigate the catalyst deactivation. In the first run red-79 dye solution of 7.14 ppm initial concentration was subjected to constant U.V. irradiation in the presence of 0.3%w virgin TiO_2 catalyst. After the completion of the process, the used catalyst was filtered and about 80-90% of the catalyst was recovered, which was reused in the second experiment with the same initial concentration of solute, i.e., 7.14 ppm. Figure 20 compares the rates of dissociation of red-79 dye for both virgin, as well as used catalyst. Figure 21 shows the effect of used catalyst on the reaction rate constant.

On the basis of reaction rate constants, the loss of activity observed was about 32%, which also includes the catalyst loss during sampling and filtration.

Some researchers at S.E.R.I. have utilized the same

catalyst as many as 30 times without any measurable loss of the activity of TiO_2 for the photo-decomposition of Trichloroethylene. For the photodecomposition process to be economically viable, it is important that the catalyst be suitable for re-use many times without deactivation.

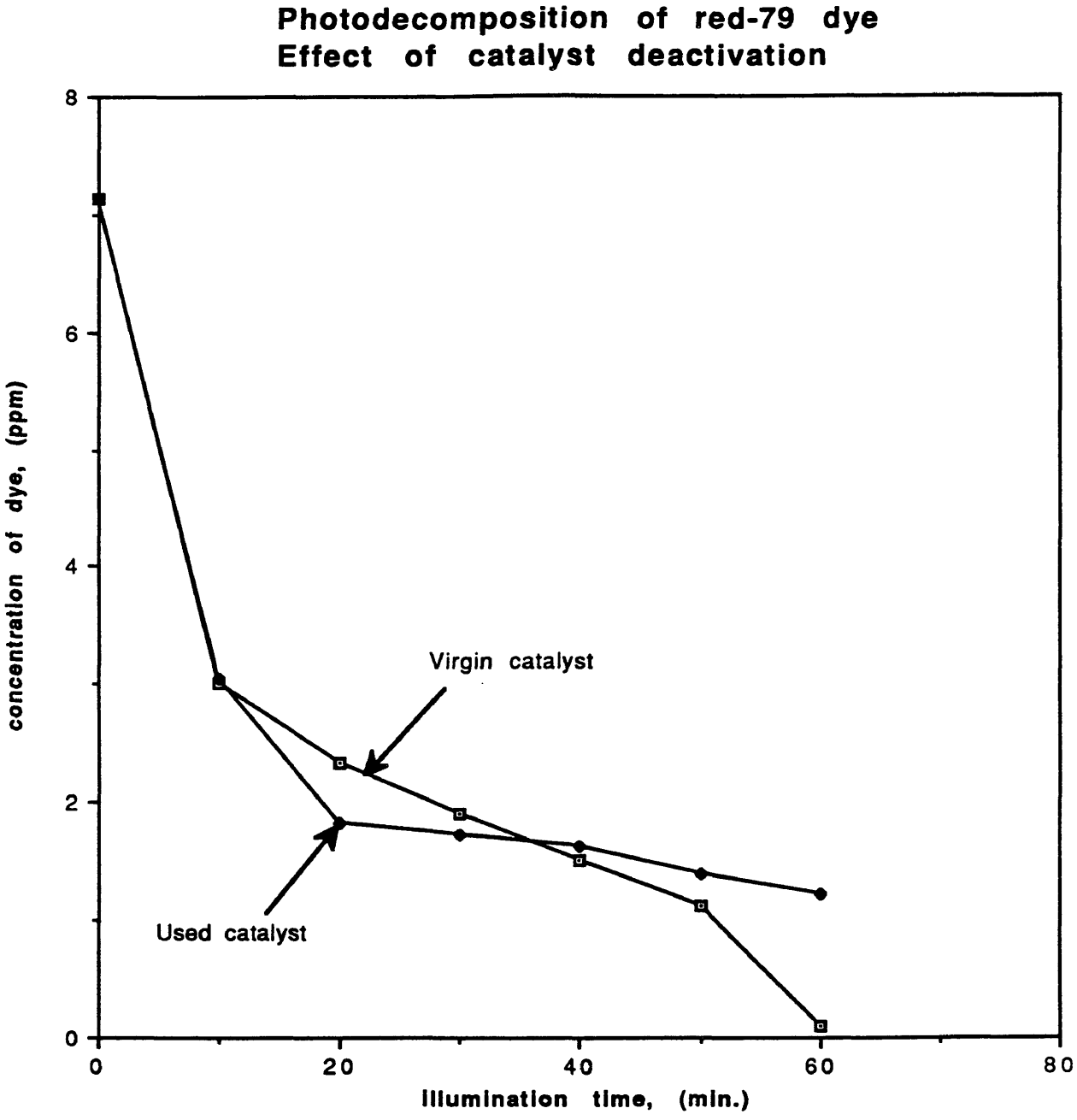

Fig. 20: Effect of catalyst deactivation on the rates of photodecomposition of red-79 dye. (Data source: Tables 3 & 4, appendix-C).

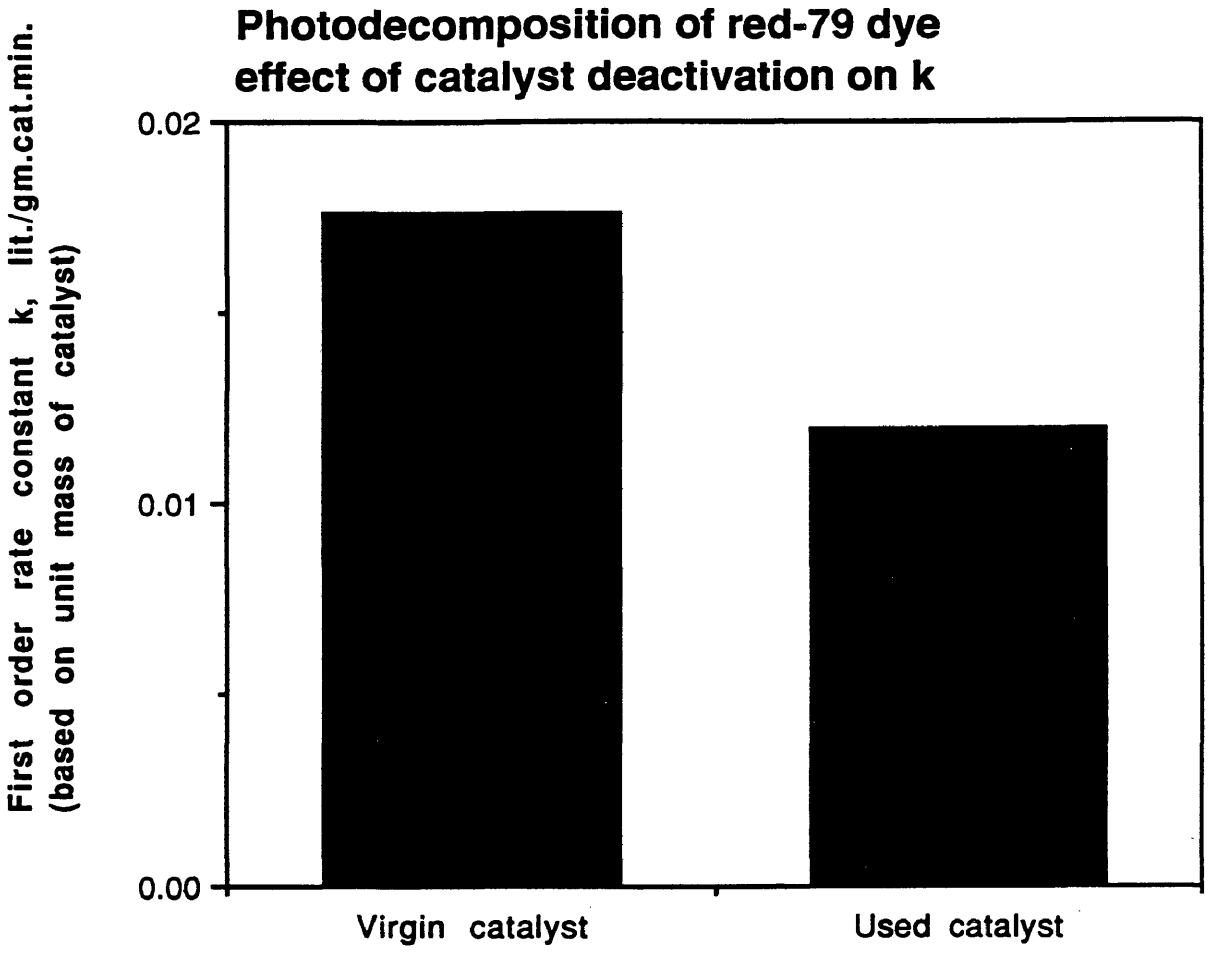

Fig. 21: Effect of catalyst deactivation on the first order rate constant k.

Comparative process economics:

In the United States the average cost per thousand gallons of water is approximately $0.20 (28). It is a relatively cheap commodity, and as result the economics of wastewater treatment is very critical. In countries where water is at a premium (e.g., Saudi Arabia, Dubai, Egypt, some parts of Pakistan like province of Sind and Baluchistan) some water treatment facilities, which are not economically justified in North America can be readily applied. In many farflung areas of the provinces of Sind and Baluchistan (Pakistan), where the people are suffering from a variety of diseases, because of the use of contaminated ground or surface water, our proposed process of Solar photodecomposition of dilute organics in aqueous streams can be successfully utilized. There is a lot of sunshine available in those areas and stand-alone solar power systems can be utilized for the energy requirements of the plant.

CONCLUSIONS

Kinetic studies have been made for the solar photodecomposition of dilute organics (red-79 dye) in aqueous streams. It was found that the water contaminated with direct red-79 textile dye can detoxified successfully using proposed process of solar water detoxification. This process can be used both for industry, as well as for mankind.

Kinetic parameters have been determined for constant U.V. intensity, as well as variable light intensity for laboratory scale, bench scale and pilot plant operations. The dependency of reaction rate constant k on the square root of the light intensity (at high light intensity) has been established for the photodecomposition process. The order of the reaction for solar photo-decomposition of red-79 dye was determined and found to be one.

Two kinetic models - first order and Langmuir-Hinshelwood were proposed, which were found compatible with experimental data. For first order model, reaction rate constant k remains constant, irrespective of the concentration of the dye. For LHHW model, k increases at lower concentration.

RECOMMENDATIONS

1). Before applying this process to a particular area, it is recommended that daily sunshine hours and solar irradiance data should be first collected.

2). This study was done using one type of pollutant (e.g, red-79 dye or blue-80 dye), studies should be made with the mixed type of pollutants in order to increase the applicability range of the process.

3). Further studies should be made to investigate the catalyst deactivation and adequate methods for the recovery of catalyst should be developed. This matter is important from the viewpoint of process economics. In this study, the catalyst was reused one time only.

4). Proper reactor design, based on the kinetics developed in this study should be carried out.

5). Optimum catalyst loading for pilot plant operation should be established for variable light intensity.

6). Studies should be done for this process in the third world countries, where water pollution is a major problem. It is recommended that the organizations such as: the World Bank, CIDA, ADB, E.E.C. should provide funding for

such type of studies especially in the African and Asian countries, where humanity is suffering from the problem of water contamination.

REFERENCES

[1] Childs, L.P. and Ollis, D.F., " Is photocatalysis catalytic" Journal of Catalysis 66 (1980): 383-390.

[2] Okamoto, K.,et al., " Heterogeneous photocatalytic decomposition of phenol over TiO_2 power " Bull. Chem. Soc. Jpn. 58 (1985): 2015-2022.

[3] Okamoto, H., et al., " Kinetics of heterogeneous photocatalytic decomposition of phenol over anatase TiO_2 powder" Bull. Chem. Soc. Jpn. 58 (1985):2023-2028.

[4] Pruden, A.L. and Ollis, D.F., " Degradation of chloroform by photoassisted heterogeneous catalysis in dilute aqueous suspensions of TiO_2 " Environ. Sci. Technol. 17 (1983):628-631.

[5] Ollis, D.F., " Contaminant degradation in water " Environ. Sci. Technol. 19 (1985):480-484.

[6] Pelizzetti, E. and Serpone, N. eds.1986 " Homogeneous and Heterogeneous Photocatalysis " Reidel Publishing Company.

[7] Nigel, J.B., et al., " An assessment of the importance of direct solar degradation of some simple chlorinated benzenes and biphenyls in the vapor phase " Environ. Sci. Technol. 23 (1989):213-218.

[8] Ollis, D.F., et al., " Heterogeneous photoassisted catalysis: Conversions of perchloroethylene, dichloroethane, chloroacetic acids and chlorobenzenes" Journal of Catalysis 88 (1984):89-96.

[9] Pruden, A.L. and Ollis, D.F., " Photoassisted heterogeneous catalysis: The degradation of trichloroethylene in water " Journal of Catalysis 82 (1983):404-417.

[10] Hsiao, C.Y., et al., " Heterogeneous photocatalysis: Degradation of dilute solutions dichloromethane, chloroform and carbon tetrachloride with illuminated TiO_2 photocatalyst " Journal of Catalysis 82(1983):418-423.

[11] Nguyen, T. and Ollis, D.F., " Complete heterogeneously photocatalyzed transformation of 1,1- and 1,2-dibromomethane to CO_2 and HBr " J. Phys. Chem. 88(1984):3386-3388.

[12] Ahmed, S. and Ollis, D.F., " Solar photoassisted catalytic decomposition of the chlorinated hydrocarbons trichloroethylene and trichloromethane " Solar Energy 32 (1984):597-601.
[13] Mathews, R.W., " Kinetics of photocatalytic oxidation of organic solutes over titanium dioxide " Journal of Catalysis 111 (1988):264-272.
[14] Kirk and Orthmer, 1988."Encyclopedia of Chemical Technology", vol.23, 5th ed. N.Y.: John Wiley.
[15] R.R. Blakey and J.E. Hall, Titanium dioxide, Technical Service department Tioxide group PLC, Central laboratories Stockton-on-Tees, England.
[16] Hewett, R., " Parabolic trough photocatalytic decmposition experimental apparatus: Engineering description and cost ", draft report, Solar Energy Research Institute, Golden, Colorado, October,1988.
[17] Sczechowski, J.G., 1987, "The role of dissolved oxygen in the photocatalytic decomposition of dilute aqueous solutions of chlorinated hydrocarbons", M.S. Thesis, Raleigh, NC, North Carolina State University.
[18] Fogler, Scott, H.,1986 "Elements of Chemical Reaction Engineering", New Jersy: Prentice-Hall.
[19] Smith, J.,M.,1983. " Chemical Engineering Kinetics " 3rd ed. N.Y.: McGraw Hill.
[20] Cassano, A.E., Matsuura, T. and Smith, J.M., "Batch, recycle reactor for slow photochemical reactions" I & EC Fundamentals 7 (1968): 655-660.
[21] Mathews, R.W. "Photooxidation of organic impurities in water using thin films of Titanium dioxide" J. Phys. Chem. 91 (1987): 3328-3333.
[22] Turchi, C.S. and Ollis, D.F., Mixed reactant photoca talysis: Intermediates and mutual rate inhibition" Journal of Catalysis 119 (1989): 483-496.
[23] Turchi, C.S. and Ollis, D.F.,"Photocatalytic degradation of organic water contaminants: mechanisms involv ing hydroxyl radical attack", Journal of Catalysis 122 (1990): 178-192.
[24] Philip, B. and Beverly, M., "Photocatalytic decomposi tion of red dye #79", unpublished report, Solar Energy Research Institute, Golden, Colorado, August, 1989.
[25] Peterson, M.W., Turner, J.A. and Nozik, A.J., "Mecha nistic studies of the photocatalytic behavior of TiO_2 particles in a photoelectrochemical slurry cell and

the relevance to the photodetoxification reactions", unpublished report, Solar Energy Research Institute, Golden, Colorado, June, 1990.

[26] Sayigh, A.A.M.,ed.1977. " Solar Energy Engineering ", N.Y.: Academic Press.

[27] Egerton, T.A. and King, C.J., "The influence of light intensity on photoactivity in TiO_2 pigmented systems", J.Oil Col. Chem. Assoc. 62 (1979): 386-391.

[28] Ramalho, R.S.,1983." Introduction to wastewater treat ment Processes ", 2nd ed. N.Y.: Academic Press.

APPENDIX A

LOG SHEET SAMPLE

APPENDIX-A.WATER DETOX EXPERIMENTAL RUN
Run parameters [page 1 of 2]

Experiment Title: _____

Storage disk no. and volume label: _____

Comments: _____

Lamp type [Xenon, Mercury, Outdoor, None] :_____
Full lamp power, I_o [watts] : _____
Actual lamp power, I_a [volts x amps., watts] : _____

Primary reflector (aluminium, dichroic) : _____

Filters [air mass, schott glass, pyrex, wire screen]: -----

Filter % transmittance at 330 nm [T]: _____

% of lamp full power [T x I_a/I_o] _____

Reaction vessel material [fused silica, pyrex]: _____

Average Temperature, ^oC:_____ Initial pH: _____

Waste material(s): _____

Initial waste concentration(s), [ppm]: _____

Calibration curve date, disk volume label and file name: __
_____

Support material: _____

Catalyst material: _____ Catalyst weight %: _____

Oxidant material: _____ Oxidant weight %: _____

Exposure time correction factor : _____

Logged by : _____ Date: _____

Reviewed by : _____ Date: _____

WATER DETOX EXPERIMENTAL RUN
Run data [page 2 of 2]

Experiment Title: _____

Storage disk no. and volume label: _____

Rate data file extension ----------|_____|_____|

Time [hr:min]	Run Time [min]	Temp. [°C]	pH	Outdoor condition	[ ] [ppm]	[ ] [ppm]

APPENDIX B

PEAK ABSORBANCE AND CALIBRATION CURVES

FOR

RED-79 AND BLUE-80 DYES

B 1. Determination of peak absorbance for direct Red-79 and Blue-80 dyes.

Red-79 dye		Blue-80 dye	
wavelength, nm.	absorbance	wavelength, nm.	absorbance
450	1.116	500	0.357
460	1.246	510	0.447
470	1.373	520	0.549
480	1.509	530	0.664
490	1.645	540	0.792
500	1.767	550	0.929
510	1.803	560	1.022
520	1.760	570	1.050
530	1.664	580	1.010
		590	0.911
		600	0.746
		610	0.563
		620	0.390

B 2. Calibration curve for Blue-80 dye

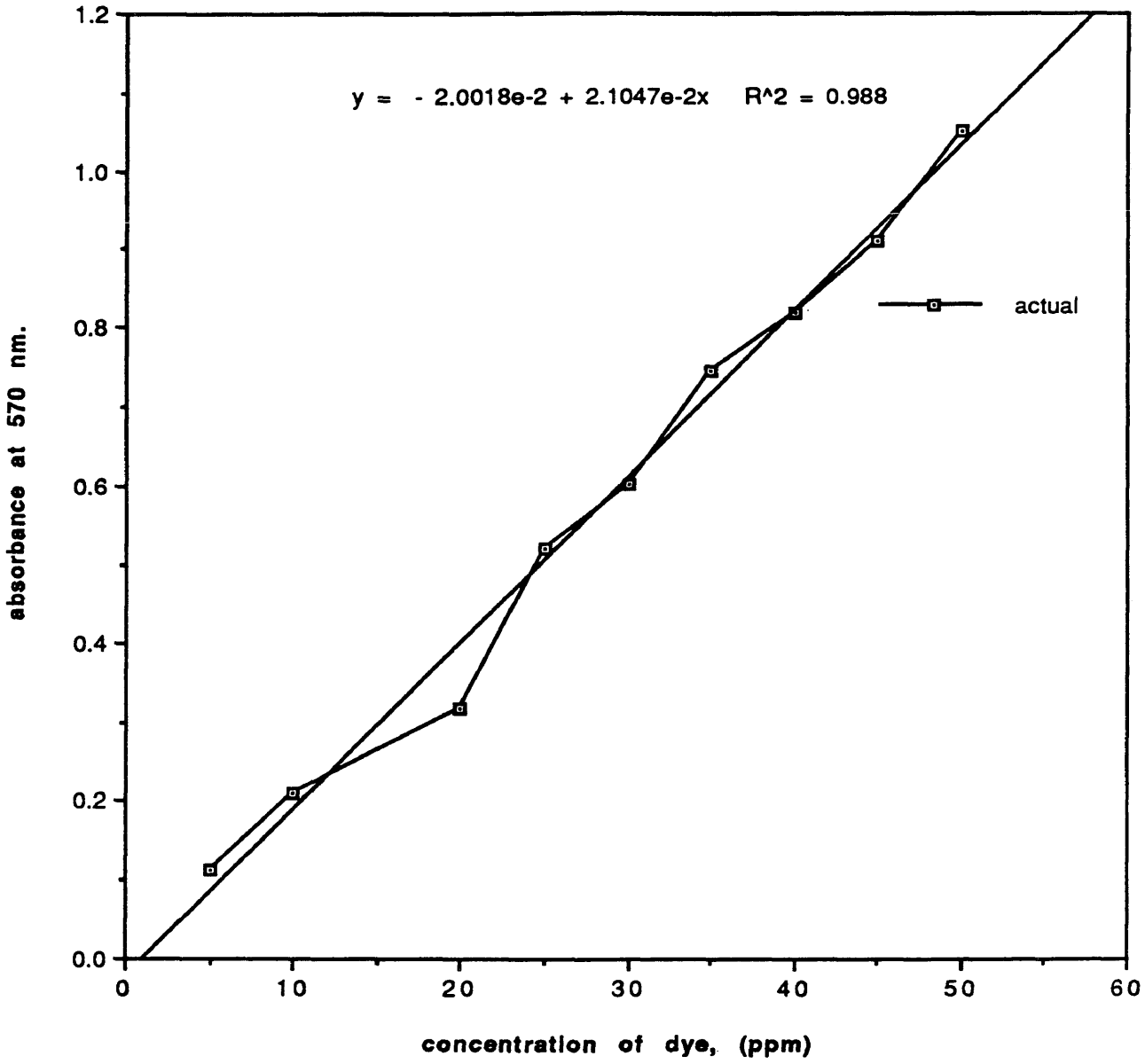

B 3. Calibration curve for Red-79 dye

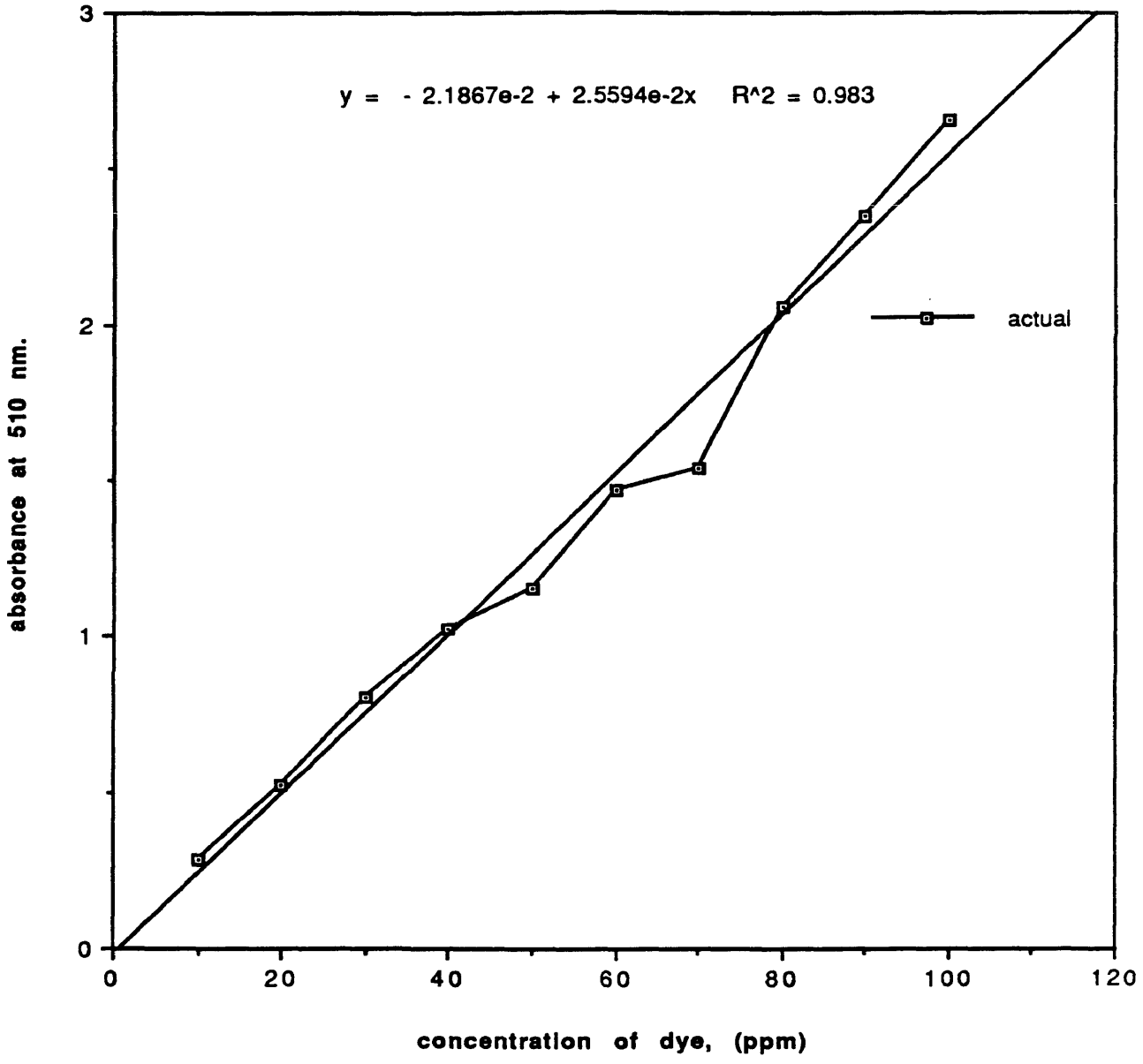

APPENDIX-C

EXPERIMENTAL DATA

Table 1: Experimental data (Laboratory scale operation to study reaction kinetics).

Initial concentration of solute (red-79 dye) = 86.19 ppm.

Volume of reactant used = 100 ml.

Mass of catalyst (Degussa P-25) used = 0.30 gm.

U.V. intensity -- constant.

Ambient temperature = 27 ^{o}C.

First order rate constant k = 0.044585 min^{-1}.

Run time (min.)	Conc. (ppm)	Temp. (^{o}C)	- dC/dt (mg./ l.min.)	ln(Co/C)
0	86.19	28	3.8377*	0
30	7.61	39	2.619333	2.427090
60	2.14	48	0.182333	3.695748
90	1.4	49	0.024666	4.120081
120	0.97	48	0.014333	4.487013

* Calculated by numerical differentiation.

Table 2: Experimental data (Laboratory scale operation to study reaction kinetics).

Initial concentration of solute (red-79 dye) = 22.30 ppm.

Volume of reactant used = 100 ml.

Mass of catalyst (Degussa P-25) used = 0.30 gm.

U.V. intensity --- constant.

Ambient temperature = 26 ^{o}C.

First order rate constant k = 0.050109 min^{-1}.

Run time (min.)	Conc. (ppm)	Temp. (^{o}C)	- dC/dt (mg./ l.min.)	ln(Co/C)
0	22.30	27	1.7853*	0
15	4.33	32	1.198	1.639019
30	3.98	39.5	0.023333	1.723304
45	2.46	42.5	0.101333	2.204425
60	1.48	44	0.065333	2.712544

* Calculated by numerical differentiation.

Table 3: Experimental data (Laboratory scale operation to study reaction kinetics).

Initial concentration of solute (red-79 dye) = 7.14 ppm.

Volume of reactant used = 100 ml.

Mass of catalyst (Degussa P-25) used = 0.30 gm.

U.V. intensity -- constant.

Ambient temperature = 25 ^{o}C.

First order rate constant k = 0.052823 min^{-1}.

Run time (min.)	Conc. (ppm)	Temp. (^{o}C)	- dC/dt (mg./ l.min.)	ln(Co/C)
0	7.14	28	0.588*	0
10	3.00	33	0.414	0.867100
20	2.34	41	0.066	1.115561
30	1.91	44	0.043	1.318609
40	1.52	44	0.039	1.547002
50	1.13	44	0.039	1.843495
60	0.10	44	0.103	4.268297

*Calculated by numerical differentiation.

Table 4: Experimental data (Laboratory scale operation to study catalyst deactivation).

Initial concentration of solute (red-79 dye) = 7.14 ppm.

Volume of reactant used = 100 ml.

Mass of catalyst (Degussa P-25) used ≈ 0.30 gm.(catalyst was reused).

U.V. intensity -- constant.

Ambient temperature = 23.5°C.

First order rate constant k = 0.035726 min^{-1}.

Run time (min.)	Conc. (ppm)	Temp. (°C)	- dC/dt (mg./ l.min.)	ln(Co/C)
0	7.14	28	-	0
10	3.04	37	0.41	0.853855
20	1.83	43	0.121	1.361396
30	1.73	44	0.010	1.417591
40	1.64	43	0.009	1.471016
50	1.40	42	0.024	1.629240
60	1.21	42	0.019	1.775092

Table 5: Experimental data (Laboratory scale operation to study reaction kinetics).

Initial concentration of solute (red-79 dye) = 68.17 ppm.

Volume of reactant used = 100ml.

Mass of the catalyst (Degussa P-25) used = 0.30 gm.

U.V. intensity -- constant.

Ambient temperature = 24.5^{o}C.

First order rate constant k = 0.072823 min^{-1}.

Run time (min.)	Conc. (ppm)	Temp. (^{o}C)	- dC/dt (mg./ l.min.)	ln(Co/C)
0	68.17	25	2.6065	0
10	42.04	27	2.613	0.483383
20	15.78	32	2.626	1.463261
30	3.74	36.5	1.204	2.902918
40	2.77	37	0.097	3.203157
50	1.99	42	0.078	3.533869
60	1.32	44	0.067	3.944372

Table 6: Experimental data (Laboratory scale operation to catalyst deactivation).

Initial concentration of solute (red-79 dye) = 68.17 ppm.

Volume of reactant used = 100 ml.

Mass of the catalyst (Degussa P-25) used ≈ 0.30 gm.(catalyst was reused).

U.V. intensity -- constant.

Ambient temperature = 26°C.

First order rate constant k = 0.048676 min^{-1}.

Run time (min.)	Conc. (ppm)	Temp. (°C)	- dC/dt (mg./ l.min.)	ln(Co/C)
0	68.17	27	-	0
10	59.77	35	0.84	0.131500
20	28.63	38	3.114	0.867549
30	23.44	42	0.519	1.067560
40	11.01	42	1.243	1.823200
50	5.27	42	0.574	2.559974
60	2.81	42	0.246	3.188820

Table 7: Experimental data (Laboratory scale operation to study reaction kinetics).

Initial concentration of solute (red-79 dye) = 74.778 ppm.

Volume of reactant used = 200 ml.

Mass of the catalyst (Degussa P-25) used = 0.60 gm.

U.V. intensity -- constant.

Ambient temperature = 24 ^{o}C.

First order rate constant k = 0.070631 min^{-1}.

Run time (min.)	Conc. (ppm)	Temp. (^{o}C)	- dC/dt (mg./ l.min.)	ln(Co/C)
0	74.778	24	4.4187	0
4	47.936	25	6.7105	0.444656
8	39.38	25	2.139	0.641265
12	31.76	27	1.905	0.856316
16	26.02	29	1.435	1.055658
20	20.468	31	1.388	1.295661
25	14.72	32	1.1496	1.625316
30	9.724	32	0.9992	2.039926
40	3.16	33	0.6564	3.163951
50	1.362	36	0.1798	4.005569
60	0.92	36	0.0442	4.397905
70	0.552	35	0.0368	4.908730
80	0.414	35	0.0138	5.196413

Table 8. Experimental data (Laboratory scale operation to study adsorption of dye on the catalyst surface).

Initial concentration of solute (red-79 dye) = 61.806 ppm

Volume of reactant used = 100 ml. (prior to operation sample was kept in dark for 24 hrs.)

Mass of the catalyst (Degussa P-25) used = 0.30 gm.

U.V. intensity --- constant.

Ambient temperature = 28^{o}C

Run time (min.)	Conc. (ppm)	Temp. (^{o}C)	- dC/dt (mg./ l.min.)	ln(Co/C)
0	61.806	28	-	0
4	37.465	28	6.08525	0.500593
8	22.461	28	3.751	1.012219
12	13.084	29	2.34425	1.55261
20	3.199	33	1.235625	2.961162
35	1.011	39	0.145866	4.11306
50	0.893	42	0.007866	4.237169
65	0.446	42	0.0298	4.931436
80	0.300	42	0.009733	5.327973

Table 9. Experimental data (Laboratory scale operation to study adsorption of dye on the catalyst surface).

Initial concentration of solute (red-79 dye) = 22.265 ppm

Volume of reactant used = 100 ml. (prior to operation sample was kept in dark for 24 hrs.)

Mass of catalyst (Degussa P-25) used = 0.30 gm.

U.V. intensity --- constant.

Ambient temperature = 28°C

Run time (min.)	Conc. (ppm)	Temp. (°C)	- dC/dt (mg./ l. min.)	ln(Co/C)
0	22.265	31	-	0
4	1.948	37	5.07925	2.436212
8	1.206	37	0.1855	2.915706
12	1.05	39	0.039	3.054225
20	0.893	40	0.019625	3.216184
35	0.595	41	0.019866	3.622209
50	0.297	41	0.019866	4.317039
65	0.15	41	0.0098	5.000135

Table 10. Experimental data (Laboratory scale operation to study effects of adding hydrogen peroxide).

Initial concentration of solute (red-79 dye) = 76.067 ppm

Volume of oxidant (Hydrogen peroxide)used = 4 ml.

Volume of reactant used = 200 ml.

Mass of catalyst (Degussa P-25) used = 0.00 gm.(no catalyst)

U.V. intensity--- constant.

Ambient temperature = 25°C

Run time (min.)	Conc. (ppm)	Temp. (°C)	- dC/dt (mg./ l. min.)	ln(Co/C)
0	76.067	25	-	0
4	75.638	26	0.10725	0.005655
8	74.739	28	0.22475	0.017612
12	73.84	30	0.22475	0.029713
16	73.645	32	0.04875	0.032358
20	73.45	33	0.04875	0.035009
35	72.082	37	0.0912	0.05381
50	71.301	42	0.052066	0.064704
65	69.347	42	0.130266	0.092491
80	68.136	43	0.080733	0.110108
95	67.315	43	0.054733	0.122231
110	65.05	43	0.151	0.156458

Table 11. Experimental data (Laboratory scale operation to study effects of adding hydrogen peroxide).

Initial concentration of solute (red-79 dye) = 75.638 ppm

Volume of oxidant (Hydrogen peroxide) used = 4 ml.

Volume of reactant used = 200 ml.

Mass of catalyst (Degussa P-25) used = 0.60 gm.

U.V. intensity --- constant.

Ambient temperature = 26°C

Run time (min.)	Conc. (ppm)	Temp. (°)	- dC/dt (mg./ l. min.)	ln(Co/C)
0	75.638	27	-	0
4	76.849	28	-0.30275	-0.01588
8	81.147	32	-1.0745	-0.07030
12	72.746	33	2.10025	0.038984
16	74.895	35	-0.53725	0.009871
20	80.287	37	-1.348	-0.05964
35	58.798	42	1.4326	0.25185
65	3.238	43	1.852	3.151002
80	1.48	43	0.1172	3.933916
95	1.167	42	0.020866	4.171522
110	0.972	42	0.013	4.354358

Table 12. Experimental data (Laboratory scale operation to studt adsorption of dye on the catalyst surface).

About ten samples of red dye solution of different initial concentrations were kept in dark for about 15 to 20 hrs.

Initial Concentration (ppm)	Final Concentration (ppm)	Change in Conc. (ppm)
0	0	0
17.77	12.576	5.194
20.625	14.994	5.631
27.267	21.115	6.152
30	23.428	6.572
35	28.40	6.60
40	32.46	7.54
50	40.57	9.43
60	48.69	11.31
65	52.75	12.25
70	56.805	13.195

Table 13. Experimental data (Laboratory scale operation to study effects of variation in light intensity).

Initial concentration of solute (red-79 dye) = 67.00 ppm

Volume of reactant used = 200 ml.

Mass of catalyst (Degussa P-25) used = 0.60 gm.

U.V. intensity --- constant.

Number of filter (s) of known transmission placed = 1

Ambient temperature = 23.5^{o}C

First order rate constant k = 0.0404 min.$^{-1}$

Run time (min.)	Conc. (ppm)	Temp. (^{o}C)	- dC/dt (mg./ l.min.)	ln(Co/C)
0	67.00	23.5	3.51644	0
5	52.04	23.5	2.99292	0.252755
10	42.31	24	1.94588	0.459737
15	33.91	25	1.68	0.681056
20	28.99	27	0.9846	0.837924
30	22.97	30	0.6017	1.070591
45	10.78	35	0.812666	1.827137
60	4.10	39	0.445466	2.794482
75	3.40	41	0.046866	2.982728
90	1.09	42	0.153666	4.119477
105	0.93	42	0.0104	4.274087
120	0.89	43	0.0026	4.316786

Table 14. Experimental data (Laboratory scale operation to study effects of variation in light intensity).

Initial concentration of solute (red-79 dye) = 65.87 ppm

Volume of reactant used = 200 ml.

Mass of catalyst (Degussa P-25) used = 0.60 gm.

U.V. intensity --- constant.

Number of filters of known transmission placed = 2

Ambient temperature = 25^{o}C

First order rate constant k = 0.0281 min.$^{-1}$

Run time (min.)	Conc. (ppm)	Temp. (^{o}C)	- dC/dt (mg./ l.min.)	ln(Co/C)
0	65.87	25.5	0.473	0
5	62.353	28	0.7034	0.054871
10	56.532	30	1.1642	0.152876
15	50.75	32	1.1564	0.260771
20	43.208	34	1.5084	0.421657
30	34.222	36	0.8986	0.654814
45	27.15	39.5	0.471466	0.886306
60	19.96	40	0.479333	1.193952
75	11.951	41	0.533933	1.706868
90	6.832	41	0.341266	2.266065
105	2.105	41	0.315133	3.443367
120	1.362	41	0.049533	3.878728

Table 15. Experimental data (Laboratory scale operation to study effects of variation in light intensity).

Initial concentration of solute (red-79 dye) = 72.278 ppm

Volume of reactant used = 200 ml.

Mass of catalyst (Degussa P-25) used = 0.60 gm.

U.V. intensity -- constant.

Number of filters of known transmission placed = 3

Ambient temperature = 25^{o}C

First order rate constant k = 0.013 min.$^{-1}$

Run time (min.)	Conc. (ppm)	Temp. (^{o}C)	- dC/dt (mg./ l.min.)	ln(Co/C)
0	72.278	25	0.039	0
5	70.129	25	0.4298	0.030183
10	64.072	26	1.2114	0.120512
15	59.696	27	0.8752	0.191254
20	56.61	28	0.6172	0.244334
30	51.921	31	0.4689	0.330796
45	37.582	34	0.9559	0.653994
60	33.556	37	0.2684	0.767304
75	30.744	37	0.1875	0.854824
90	21.440	37	0.6203	1.215261
105	17.851	37	0.2393	1.398460
120	14.725	37	0.2084	1.590973

Table 16. Experimental data (Laboratory scale operation to study effects of variation in light intensity).

Initial concentration of solute (red-79 dye) = 71.965 ppm

Volume of reactant used = 200 ml.

Mass of catalyst (Degussa P-25) used = 0.60 gm.

U.V. intensity --- constant.

Number of filters of known transmission placed = 4

Ambient temperature = 27^{o}C

First order rate constant k = 0.00567 min.$^{-1}$

Run time (min.)	Conc. (ppm)	Temp. (^{o}C)	- dC/dt (mg./ l.min.)	ln(C/Co)
0	71.965	27	0.1134	0
5	71.535	27	0.086	0.005993
10	71.379	27	0.0312	0.008176
15	68.253	28	0.6252	0.052958
20	66.104	28.5	0.4298	0.084950
30	63.291	31	0.2813	0.128436
45	60.517	34	0.1849	0.173255
60	53.875	37	0.4428	0.289513
75	47.741	39	0.4089	0.410389
90	43.677	40	0.2709	0.499358
105	37.660	41	0.4011	0.647581
120	34.534	43	0.2084	0.734235

Table 17 Experimental data (Pilot plant operation to study reaction kinetics).

Run date: September 27,1989.

Initial concentration of solute (red-79 dye) = 51.53 ppm.

Volume of reactant used = 10 gal. (38 lit.)

Mass of catalyst (Degussa P-25) used = 114.0 gm.

U.V. intensity = variable

Ambient temperature = $27^{o}C$

First order rate constant k = 0.0221 $min.^{-1}$

Time	Run time (min.)	Conc. (ppm)	Outdoor condition	-dC/dt	ln(Co/C)
10:00	0	51.530	partly cloudy	-	0
10:15	15	37.933	hazy	0.90646	0.306337
10:45	45	22.774	sunny with haze	0.50532	0.816566
11:15	75	13.318	sunny with haze	0.31517	1.353029
11:30	90	7.067	sunny with haze	0.41676	1.986751
11:45	105	4.214	sunny with haze	0.19014	2.503603
12:00	120	2.534	sunny with haze	0.11200	3.012145
12:15	135	1.870	sunny with haze	0.04428	3.316041
12:30	150	1.480	sunny with haze	0.02604	3.550371
12:45	165	1.323	cloudy	0.01041	3.662000
13:00	180	1.167	partly cloudy	0.01041	3.787675
13:15	195	1.050	partly sunny	0.00781	3.893520

Table 18 Experimental data (Pilot plant operation to study reaction kinetics).

Run date: November 22,1989.

Initial concentration of solute (blue-80 dye) = 24.517 ppm.

Volume of reactant used = 10 gal. (38 lit.)

Mass of catalyst (Degussa P-25) used = 114.0 gm.

U.V. intensity = variable

Ambient temperature = 25 ^{o}C

First order rate constant k = 0.00945 $min.^{-1}$

Time	Run time (min.)	Conc. (ppm)	Outdoor condition	-dC/dt	ln(Co/C)
10:00	0	24.517	sunny	-	0
10:15	15	21.524	hazy	0.19953	0.130209
10:30	30	20.479	partly cloudy	0.06968	0.179991
10:45	45	16.440	sunny	0.26920	0.399650
11:00	60	13.494	sunny	0.19640	0.597103
11:15	75	11.499	sunny	0.13300	0.757129
11:30	90	9.503	sunny	0.13300	0.947734
11:45	105	8.363	sunny	0.07600	1.075555
12:00	120	7.223	sunny	0.07600	1.222142
12:15	135	6.225	sunny	0.06480	1.370806
12:30	150	5.940	sunny	0.02066	1.417683
13:00	165	5.322	sunny	0.04120	1.527481
13:15	180	4.514	sunny	0.05386	1.692075
13:30	195	4.087	sunny	0.02853	1.791584
13:45	210	3.232	sunny	0.05700	2.026369
14:00	225	2.804	sunny	0.02583	2.168299
14:15	240	2.519	sunny	0.01900	2.275510
14:30	255	2.376	sunny	0.00946	2.333758
14:45	270	2.091	sunny	0.01900	2.461542

Table 19 Data for initial rates, to be used for the determination of kinetc parameters for LHHW model (Laboratory scale operation under constant U.V. condition).

Initial conc. C_{ao}, mg./lit.	Initial rate r_{ao}, mg/lit.min.
7.14	0.588
22.30	1.7853
68.17	2.6065
74.778	4.4187
86.19	3.840

APPENDIX-D

MISCELLANEOUS DATA

Table 1. Experimental data for catalyst loading.

Run time (min.)	Catalyst loading		
	0.1%w TiO_2	0.2%w TiO_2	0.3%w TiO_2
	k = 0.0057	k = 0.0159	k = 0.0243
	Conc. (ppm)	Conc. (ppm)	Conc. (ppm)
0	62.50	67.00	68.17
10	-	-	42.04
20	-	-	15.78
30	48.50	-	3.74
35	-	37.50	-
40	-	-	2.77
50	-	-	1.99
60	48.50	-	1.32
75	-	20.00	-
90	42.00	-	-
135	-	9.00	-

Table 2. U.V. intensity data.

U.V.intensity, I (w/m^2)	Sq.rt. I	rate const.(expt.)	k (model)
343.176	18.52501	0.0706	0.072816
214.4858	14.64533	0.0404	0.037605
167.1921	12.93028	0.0281	0.02204
146.514	12.1043	0.013	0.014544
136.6125	11.68814	0.00567	0.010767